N O T I C E

THIS DOCUMENT HAS BEEN REPRODUCED FROM MICROFICHE. ALTHOUGH IT IS RECOGNIZED THAT CERTAIN PORTIONS ARE ILLEGIBLE, IT IS BEING RELEASED IN THE INTEREST OF MAKING AVAILABLE AS MUCH INFORMATION AS POSSIBLE

NASA

Technical Memorandum 83829

Predictability of the Tropical Atmosphere

(NASA-TM-83829) PREDICTABILITY OF THE TROPICAL ATMOSPHERE (NASA) 57 p HC A04/MF A01 CSCL 04B

N82-19775

Unclas

G3/47 13971

J. Shukla

October 1981

Laboratory for Atmospheric Sciences
Modeling and Simulation Facility

MAR 1982
RECEIVED
NASA STI FACILITY
ACCESS DEPT.

National Aeronautics and
Space Administration

Goddard Space Flight Center
Greenbelt, Maryland 20771

Predictability of the Tropical Atmosphere

J. Shukla

Laboratory for Atmospheric Sciences
NASA/Goddard Space Flight Center
Greenbelt, Maryland 20771

CONTENTS

1. Abstract

2. Introduction

3. Part I: Short range predictability of the tropical atmosphere

4. Part II: Predictability of monthly and seasonal means for tropics

5. Part III: Influence of tropical forcing on the circulation of the extra-tropical atmosphere

6. Summary, Conclusions and Suggestions

ABSTRACT

An examination of the deterministic predictability for tropics and middle-latitudes separately indicates that the theoretical upper limit of deterministic predictability for low latitudes is shorter than that for middle latitudes. Most of the day-to-day fluctuations in the tropics are determined by the growth and decay of condensation driven instabilities for which the amplitudes get equilibrated rapidly. The errors of observations are already closer to the maximum possible error for useful predictability. Therefore it takes only a few days for an initial error to grow to a magnitude comparable to the climatological variance.

Variability of time averages in low latitudes is mainly determined by the location and intensity of the large-scale Hadley and Walker circulations. Since these are largely influence by the slowly varying boundary conditions of sea surface temperature and soil moisture, and since synoptic instabilities are not strong enough to change drastically the large scale flow, therefore, there is larger potential for predictability of monthly and seasonal means in low latitudes. Since the tropical heat sources can also influence the variability of the middle latitude circulations, under favorable conditions, time averages for middle latitudes can also be potentially predictable due to their interaction with the tropical heat sources.

It is conjectured that for short and medium range deterministic prediction, a prescribed diabatic heating field due to moist convection may be more useful than their explicit calculation from the evolving flow. Inadequacies of the current parameterization techniques rapidly degrade the motion field, which in turn produces more unrealistic heating fields giving rise to still more unrealistic flow patterns.

Introduction:

The theoretical upper limit for deterministic prediction is mainly determined by the growth rate and equilibration of dominant instabilities which exist for a given observed state of the atmosphere. An uncertainty in the initial conditions grows with the characteristic growth rate of the fastest growing instabilities. Nonlinear interactions among different scales of motion help spread this instability to all the scales present in the flow. For a simple hydrodynamical system (barotropic fluid without β effect and without mountain), Lorenz (1969) showed that different scales of motion have different ranges of predictability and that the theoretical upper limit of predictability ranges from a few days to a few weeks. Several general circulation model studies have been carried out (Charney et al., 1966; Smagorinsky, 1969) to determine the theoretical upper limit of predictability. In these studies a general circulation model is first integrated with observed (or model simulated) initial conditions. Initial conditions are then perturbed by superimposing a random field of meteorological variables, and the model is integrated again keeping everything (boundary conditions, physical parameterizations, model, etc.) identical to the first run. Random perturbations in the initial conditions are assumed to simulate uncertainty in the definition of the initial state[1]. Departures beween the two model integrations are studied as a function of time to determine the growth rate of errors. On the basis of the rate of growth of the globally averaged root mean square error, it has been suggested that the doubling time for the error is about three to five days. It should be noted that this approach only gives an estimate of the doubling time, and in order to determine the upper

---

[1] The inadequacy of the present observing systems gives rise to, in addition to random errors, large systematic errors over the data-void areas.

limit of predictability, one must assume a value for the initial error and another value for the final tolerable error.

In this paper, we have shown that the error growth rates and their equilibration depend upon the dynamical regime, the magnitude of the error, the initial condition, and the meteorological variable. Since the nature of dynamical instabilities which re most important for day-to-day fluctuations in the tropics are very different from those in the middle latitudes, it is not appropriate to examine the growth rate of combined error. In fact, even in the middle latitudes, it is reasonable to assume that the growth rates in the regions of highly active storm-tracks will be larger than those in the regions of quasi-permanent anticyclones. These arguments are valid only for initial growth rates and subsequently error growth rates will also be determined by interaction among different scales and different dynamical regimes. For example, for a suitable structure of the zonal flow, middle latitude effects can propagate to the lower latitudes and vice-versa, and for time periods longer than the time scale of these interactions, one must consider the combined effects.

The tropical circulation is dominated by quasi-stationary heat sources and associated Hadley and Walker type circulations. The space and time scales of these circulations are much larger than the space and time scales of tropical disturbances (easterly waves, depressions, cyclones, etc.). Therefore it is less likely that the large scale tropical circulations can be made unpredictable by their interaction with the small scale tropical disturbances. Although there is evidence to suggest that the initiation of the tropical disturbances is mainly due to dynamical instabilities (barotropic or combined barotropic-baroclinic), it is well known that the further growth and the maintenance of tropical disturbances is mainly due to the latent heat of condensation, and CISK is the most dominant dynamical mechanism to explain their energetics.

The maximum amplitude of these disturbances is equilibrated by availability of moisture and efficiency of utilizing the available moisture (Stevens et al., 1977; Shukla, 1978). Formation, growth and movement of these disturbances is very important for short-range forecasting in the tropics. Condensation driven instabilities (CISK) have large growth rates but their amplitudes equilibrate rather quickly. This unique nature of tropical disturbances can be a major obstacle for short-range prediction in the tropics. Since the spatial scale of these disturbances is only about 2000-3000 km and embedded cloud clusters are even smaller, it is required to have a sufficiently high resolution to define their structure.

The fluctuations of large-scale Hadley and Walker circulations are affected by the slowly varying boundary conditions of sea-surface temperature (SST) and soil moisture. It is therefore conceivable that the time averages (at least for the time scales over which SST and soil moisture do not change rapidly) of the tropical circulation may be more predictable. Changes in SST can change the location of ascending branches of the Hadley and Walker cells and structure of diabatic heating fields and therefore produce large changes in the time averaged precipitation and associated circulation. For longer time scales one must also consider the interaction between tropical and middle latitude circulations. Fluctuations in momentum and heat fluxes due to middle latitude eddy activity can affect the intensity of Hadley circulation and if the former are unpredictable, the latter would also be unpredictable. Based on the above considerations, Charney and Shukla (1981) suggested that the time-averaged monsoon circulations are more predictable than the time-averaged middle latitude circulation.

The middle latitude circulation is dominated by stationary planetary waves forced by orography and diabatic heat sources, transient long waves and

baroclinically unstable synoptic scale waves. Fast growing baroclinic instabilities interact with the larger scales and make them unpredictable. Prediction of time averages (viz. for monthly means) for middle latitudes, therefore, is more difficult than for low latitudes. Unlike the tropical case, the interaction between baroclinic eddies and planetary waves in the middle-latitudes is much stronger and therefore the potential for long range predictability is smaller.

However, the potential for short range deterministic prediction in middle latitudes is much better than that for the low latitudes. The maximum amplitude of equilibration for middle latitude eddies is large enough so that the initial uncertainty has to grow for several days before it becomes comparable to the magnitude of the day-to-day fluctuations we wish to predict.

In Part I of this paper we have utilized the GLAS (Goddard Laboratory for Atmospheric Sciences) climate model to examine the growth rate for initial random errors for low and middle latitudes separately. We have also compared the errors due to random perturbation with the maximum tolerable error (given by the standard deviation of the total time series) for each grid point and presented the results of zonal averages. It is found that for a reasonable value of the initial error, the error becomes about half of the maximum error within 2-3 days for the tropics and 5-7 days for the middle latitudes.

In Part II of this paper we have examined the effects of SST fluctuations between the equator and 30°N. We find support for the hypothesis proposed by Charney and Shukla (1981) that the fluctuations of the boundary conditions can explain a significant part of the interannual variability of the tropical atmosphere. We have examined the effects of SST fluctuations between the equator and 30°N. It is found that the interannual variability of SST can explain a significant part of the variability of the tropical atmosphere.

In Part III of this paper we have summarized the results of numerical experiments carried out with global general circulation models which suggest the importance of boundary conditions for predictability of the time-averaged tropical circulation.

Finally, we have conjectured that it is the quasi-steady components of the tropical heat sources which are important in affecting the circulation over middle latitudes, and therefore, although the tropical atmosphere itself is deterministically unpredictable for short and medium range, its influences on middle latitudes could be calculated by prescribing the observed structure and intensity of the tropical heat sources.

Random error, Climatological error and Persistence error.

For a time series x_t (t=1,2,...N), the variance (σ^2) is defined as

$$\sigma^2 = \frac{1}{(N-1)} \sum_{1}^{N} (x_t - \bar{x})^2 \qquad \text{where } \bar{x} = \frac{1}{N} \sum x_t$$

If E^2 is the mean square difference between all possible pairs of x_t, it can be shown that

$$E = \sqrt{2}\,\sigma$$

E is a statistical measure of error between two randomly chosen values and σ is a statistical measure of error if the long term mean (climatology) was assumed to be the forecast for each day. These definitions remain valid both for a point (station) and for a spatial domain. The persistence error at any point changes with time and the magnitude of the error depends upon day-to-day atmospheric fluctuations. E at any point, for sufficiently large samples, can be a statistical measure of persistence error because it then becomes equivalent to using all possible pairs. Alternatively, if the persistence error is calculated over a spatial domain with a large number of points—large enough so that the spatial distribution of error at any time is comparable to the time distribution of error of all the points--the maximum value of persistence error can be estimated by E. The persistence error grows rapidly for a few days before it attains its maximum value. In the absence of a long time series, the maximum value of persistence error can be used to estimate the climatological standard deviation.

The theoretical upper limit of predictability is generally considered to be the time taken for the error to be comparable to the error between two randomly chosen model states. Since this error is $\sqrt{2}$ times larger than the standard deviation of a climatological forecast, which does not require any

skill in prediction, it is too large an error to be a measure of useful prediction. In this paper, we shall assume σ to be the maximum tolerable error for calculating the limits of predictability. It is known that the standard deviations of day-to-day fluctuations have a well defined geographical structure, in particular, σ at low latitudes is smaller than that at middle and high latitudes. It is therefore more appropriate to estimate predictability by comparing the magnitude of prediction error and σ at each point separately.

The upper limit of predictability is determined by the relative magnitudes of the error growth rate and the maximum day-to-day variability. If the growth rate is small, it takes longer for the error to be comparable to the maximum error; if variances due to day-to-day fluctuations are small, it takes only a few days for the error to be comparable to the maximum error. However, the error growth rate itself is not constant with time. Small errors grow more rapidly than the large errors. Therefore, a smaller growth rate does not necessarily imply longer predictability because small growth rate can be simply due to the fact that the error is already close to its maximum value.

Part I. Short range predictability of the tropical atmosphere.

We have examined the error growth among four general circulation model runs for which the initial conditions were randomly perturbed. The model was first integrated for 45 days starting from the initial conditions of middle of June. Three additional runs were made by perturbing the initial conditions of sea level pressure, U, V, and T at each of the nine levels of the model. Each grid point was randomly perturbed corresponding to a gaussian distribution with zero mean and standard deviation of 3 m/s for u and v, 1°C for T and 1 mb for sea level pressure. It should be noted that these errors of present observing system are comparable to day-to-day fluctuations of the tropical flow. The boundary conditions were identical for all the four model integrations. We have calculated the standard deviation among the four runs at each grid point for each day. These model runs were carried out by Charney et al. (1977) and designated as predictability runs in their paper.

If any variable R for model run m at grid point i,j at time t is denoted as $R_{i,j,t,m}$ we calculate the error (e) among the four runs as follows:

$$e_{i,j,t} = \left[\sum_{m=1}^{M} (R_{i,j,t,m} - \bar{R}_{i,j,t})^2/(M-1) \right]^{1/2}, \quad (M=4)$$

where $(\bar{R}) = 1/M \sum_{m=1}^{M} (R)$ is the average for the four runs.

We have also calculated the standard deviation (s) at each grid point among all the model states realised during 45-day integration of the four runs.

$$s_{i,j} = \left[(1/180) \sum_{m=1}^{4} \sum_{t=1}^{45} (R_{i,j,t,m} - R_{i,j,t})^2 \right]^{1/2}$$

s is a measure of the error of a climatological forecast. We would consider the upper limit of predictability to be the time taken for e to be comparable to s.

Figures 1a and 1b show the evolution of the errors for sea level pressure and U at 175 mb, respectively. In each figure, the solid line, dashed line and dotted line refer to the error average over the 10° latitude belts centered at 6°N, 30°N and 58°N, respectively. It is seen that the error in the zonal velocity at the end of one day is largest at 6°N, followed by 30°N and 58°N. The same was true for the meridional velocity at 835 mb (not shown). The final values of error for U at 175 mb at 6°N, 30°N and 58°N are comparable because during the summer the zonal velocity and its fluctuations at this level are very large for all the three latitudes; at 6°N due to an easterly jet stream and at 30°N due to a subtropical jet stream. The final values of error for V at 835 mb (not shown) were comparable for 6°N and 58°N. This is because the middle latitude summer circulation is not as vigorous as the winter circulation and the day-today fluctuations in meridional velocity are not as strong. The final value of error for sea-level pressure is smallest at 6°N and largest at 58°N. This is due to small day-to-day fluctuations of sea level pressure in the tropics and larger day-to-day fluctuations in the middle latitudes.

Figures 2a, 2b, and 2c show the zonally averaged values of the ratio (e/s) for the zonal velocity (U) at 175 mb, zonal velocity (U) at 835 mb and sea level pressure respectively. In each figure the zonal average of the ratio (e/s) is shown for day 1, day 2, day 3 and day 7. The following conclusions for summer emerge from these figures.

i) The error in the tropics becomes half of the climatological standard deviation within 2-3 days, whereas, for middle-latitudes, it takes about 5-7 days.

ii) The error growth rate for sea level pressure is different from that for wind. In the tropics, the error in sea level pressure reaches its maximum value much faster than that in the winds. The same is true for the temperature (not shown). This, of course, also depends upon the magnitude of the initial error and the magnitude of s which depends upon the time variability of the parameter under consideration. Fluctuations of pressure and temperature are rather small in the tropics.

Smaller values of s in the tropics suggests that the day-to-day fluctuations are not as large as in the middle-latitudes. In the tropics, the errors of observation are already closer to the maximum permissible error for useful predictability and therefore it takes only a few more days for the error to be equal to the maximum error.

Figure 3 shows the zonally averaged values of doubling time for different latitudes. The doubling time for the low latitudes is about 4-10 days which is higher than that for the middle and high laitudes. In particular, sea level pressure shows the largest doubling time in the tropics. This does not mean that the tropics have longer predictability because, as discussed earlier, the doubling times are larger because the errors are already close to their maximum value. It can be seen from Figures 2a, 2b, 2c that the predictability is smallest for sea level pressure compared to U at 175 mb and 855 mb.

We have repeated these calculations for the version of the GLAS model described by Halem et al. (1980). Starting from the initial conditions in the middle of June, the GLAS model was first integrated for 90 days. A second integration for 90 days was also carried out in which only initial conditions of U and V fields at all the nine levels of the model were randomly perturbed. Each grid point was randomly perturbed corresponding to a Gaussian distribution with zero mean and standard deviation of 3 m/sec for U and V fields. Figures 4a, 4b, 4c and 4d show the evolution of the initial error for sea level pressure, U, V and T at 500 mb, respectively. In each figure, the solid line, dashed line and dotted line refer to the error averaged over a 10° latitude belt centered at 6°N, 30°N and 58°N, respectively. It should be noted that although there was no initial error in the temperature and pressure field, the error in these fields for the first 4-5 days is the largest at 6°N. The same is true for errors in U and V components. This suggests that the rate of

growth of initial error is large in the tropical latitudes compared to the middle latitudes. The final asymptotic value of the errors in sea level pressure and 500 mb temperature field is the largest for 58°N and the smallest for 6°N. This is due to large day-to-day fluctuations in sea level pressure and temperature in the middle laitudes compared to the low latitudes. Due to the smallness of coriolis parameter, large changes in pressure and temperature cannot be sustained in the tropics. The large values of the final error in U and V components are due to the subtropical jet stream near 30°N and tropical jet stream near 6°N during the northern summer.

We have also calculated the error growth rate and predictability of the GLAS model for winter initial conditions. Figure 5a shows the zonally averaged root mean square error for geopotential height for nine pairs of model integrations in which the winter initial conditions of U and V at nine levels of the GLAS model were randomly perturbed. It is seen that the error in the tropics is the smallest and the error in the northern hemispheric middle and high latitudes is the largest. The error in the southern hemisphere (summer) middle latitudes is larger than the tropics but not as large as the northern hemisphere (winter) middle latitudes. Figure 5b shows the zonal average of the ratio of the error and standard deviation of day-to-day fluctuations. It is seen that the ratio is large for the low latitudes compared to the middle latitudes. This indicates that although the error is smaller for the low latitudes, the magnitude of the day-to-day fluctuations is so small that it takes only a few days for the error to be about half of the standard deviation.

The above results suggest that the short term predictability for the tropical atmosphere is limited only to a few days because of two reasons: the rate of growth of the initial error is large and the maximum possible value of error is small. If the initial errors (due to observational errors, lack of

observations or deficiency of analysis and intialization schemes) were comparable for the low and the middle latitudes, the limit of predictability for the low latitudes will be lower even if the growth rates were comparable. There is reason to believe that, since the low latitude instabilities are driven mainly by condensation, they would be relatively more unpredictable because of the limitations on the physical parameterization of moist convective processes. This, we believe, is especially true for the northern summer when moist convection is very important in determining the nature of day-to-day fluctuations. This would suggest that the results of such predictability studies, and therefore also the results of actual numerical prediction, will depend upon parameterization of physical processes of moist convection, boundary layer processes and cloud-radiation interactions. The spatial scale of the tropical easterly waves and depressions is also smaller than that of mid-latitude baroclinic eddies and thus they require higher resolution for defining their structure. Even higher resolution would be required to define the mesoscale structures embedded in the tropical disturbances. On the other hand, for middle latitude disturbances, a quantitative treatment of the main energetic processes of conversion from available potential energy to kinetic energy is more reliable because it depends upon the large-scale vertical velocity and temperature fields.

Based on these considerations alone, it can be inferred that even for an idealized case of a uniform and high density of observations over the globe, the upper limit of deterministic predictability will be shorter for the tropics than for the middle latitudes. The reality of the situation is, of course, much worse. Tropical areas, even in the northern hemisphere, have far less upper air soundings compared to the northern hemispheric middle latitudes.

An additional important problem for short range predictability is related to the treatment of mountains. Inadequate treatment of large-scale orographic effects (stationary forcing on a planetary scale) and small scale effects (lee cyclogenesis, flow over and around mountains) is one of the serious deficiencies of present NWP models. Although these effects are important both at low latitudes and middle latitudes, it is more difficult to treat the interaction of local topography and tropical disturbances which are primarily driven by condensation.

Part II. Predictability of monthly and seasonal means for tropics.

The interannual variability of monthly and seasonal means is determined by the combined effects of the internal atmospheric dynamics and the slowly varying 'external' boundary conditions of sea surface temperature (SST), soil moisture, snow/sea ice, etc. Although solar heating is the only truly external forcing to the atmosphere, the boundary conditions at the earth-atmosphere interface can be assumed to be external at least for those time scales for which they change slowly compared to the atmospheric dynamics. There is observational evidence to suggest that these boundary conditions in fact do change slowly enough so that they may be thought of as constant in time up to even a season, which is a longer time scale compared to the time scale of synoptic scale instabilities which are most important for day-to-day fluctuations. In the absence of any changes in these boundary conditions, the internal dynamical changes (which include the earth's topography and the land-sea contrast) will produce interannual variability of monthly and seasonal means. If the total interannual variability could be explained by the internal dynamics alone, the potential for predictability of time averages would be rather low. It is difficult to isolate the contribution of these two factors because the boundary conditions themselves are affected by the atmospheric dynamics, and observed variability is due to complex interaction between the two (Straus and Halem, 1981). Realistic physical models of the atmosperic circulation can be useful in conducting controlled numerical experiments to determine the relative roles of internal dynamics and boundary conditions.

Charney and Shukla (1981) have suggested that the time-averaged monsoon circulation is potentially more predictable than the middle latitude circulation. This is so because the large-scale monsoon circulation is stable with respect

to dynamic instabilities which develop in the monsoon flow, and fluctuations in the boundary conditions have significant effects on the time-averaged monsoon flow. This conclusion was arrived at by examining the variability among the monthly mean (July) circulations of four model runs for which the boundary conditions were kept identical but the initial conditions were randomly perturbed. It was found that, although the observed and the model variabilities were comparable for middle and high latitudes, the variability among the four model runs for the monsoon regions was far less than the observed interannual variability of the atmosphere. This led us to conclude that the remaining variability could be due to the boundary conditions. This was also consistent with the results of several observational studies and numerical experiments which showed that the changes in SST or soil moisture at low latitude produce significant changes in the atmospheric circulation.

In this paper we have extended the work of Charney and Shukla (1981) by comparing the model variability due to internal dynamics and due to changes in the boundary condition of SST. One of the limitations of the earlier study was the comparison of the model variability with the observed variability. While this must be the ultimate goal, it is more appropriate first to intercompare two different properties of the same model so that any deficiencies of the model itself do not bias the conclusions.

We have carried out a 45-day integration of the GLAS model starting from the observed initial conditions in the middle of June, and climatological mean boundary conditions of SST. We refer to this integration as control run (c). For the identical boundary conditions we have carried out three additional integrations for 45 days each by randomly changing the initial conditions of u and v at each of the nine levels of the model. The spatial structure of the random errors corresponded to a Gaussian distribution with zero mean and standard

deviation of 3 m/s for u and v separately. We refer to these three integrations as predictability runs (P_1, P_2, and P_3). Although the statistical properties of the random errors were the same for each predictability run, the actual grid point values were randomly different. We have also carried out three additional integrations for which, in addition to the randomly perturbed initial conditions, the boundary conditions of SST between the equator and 30°N were replaced by the observed[3] SST during July of 1972, 1973, 1974. We refer to these three integrations as boundary forcing runs (B_1, B_2, and B_3). The differences between the climatological SST as used in the control and predictability runs, and the observed SST used in boundary forced runs is shown in Figures 6a, 6b, and 6c. Although there are large systematic differences over a few grid points, the SST anomaly over most of the tropical oceans appears to be realistic.

The variance $(\sigma_p)^2$ among C, P_1, P_2, and P_3 will give a measure of the natural variability of the model; the variance $(\sigma_B)^2$ among C, B_1, B_2, and B_3 will give a measure of the variability due to changes in the boundary conditions of tropical SST. We have also calculated the observed variances $(\sigma_o)^2$ for ten years of observed monthly means.

$$(\sigma_p)^2_{i,j} = 1/3 \left[(C - \overline{P})^2 + (P_1 - \overline{P})^2 + (P_2 - \overline{P})^2 + (P_3 - \overline{P})^2 \right]_{i,j}$$

$$(\sigma_B)^2_{i,j} = 1/3 \left[(C - \overline{B})^2 + (B_1 - \overline{B})^2 + (B_2 - \overline{B})^2 + (B_3 - \overline{B})^2 \right]_{i,j}$$

where $\overline{P} = (C + P_1 + P_2 + P_3)/4$

and $\overline{B} = (C + B_1 + B_2 + B_3)/4$

where C_{ij}, P_{ij}, B_{ij} denote the July mean at grid point ij.

Figure 7 shows the plots of zonally averaged values of standard deviations σ_p, σ_B, σ_o and the ratios σ_o/σ_p and σ_o/σ_B. In agreement with the results of Charney and Shukla (1981), it is seen that the ratio σ_o/σ_p is more than

---

[3] The observed SST was kindly provided to us by Dr. E. Kraus.

two in the tropical latitudes and close to one in the middle latitudes. The new result is that the curve σ_B lies nearly halfway between the curves σ_O and σ_P, This suggests that about half of the remaining variability for this model is accounted for by changes in sea-surface temperature between equator and 30°N.

This supports our earlier hypothesis that the slowly varying boundary conditions play an important role in determining the interannual variability of time averages for the tropics. Additional effects of soil moisture or the Eurasian snow cover could possibly bring the σ_O and σ_B curves still closer. It is however to be noted that the long period internal dynamical changes (tropical-extratropical interactions, etc.) also contribute to the interannual variability of time averages and it could never be possible to explain the total σ_O by boundary conditions alone. In one of the model integrations for 90 days described in the earlier section, it was found that large differences in the monthly means were produced by internal dynamics alone.

We have also compared the model variability for the predictability and boundary forcing runs. Since the sea surface temperature anomalies for B_1, B_2, and B_3 have many common features, we have considered it more appropriate to calculate the changes in the monthly means due to boundary conditions (E_B) and due to random perturbations (E_p) as follows:

$$E_B^2 = 1/3 \sum_{k=1}^{3} (C - B_k)^2 \qquad \text{(at each grid point i,j)}$$

and

$$E_p^2 = 1/3 \sum_{k=1}^{3} (C - P_k)^2 \qquad \text{(at each grid point i,j)}$$

Figure 8 shows the zonally averaged values of E_B and E_p for July mean geopotential height at 300 mb. Curves for E_p and E_B are labeled as 'PREDICTABILITY' and 'SST ANOMALY' respectively. As is well known, the values of E_B and E_p are small for the low latitudes and large for the middle latitudes, however, the

ratio E_B/E_p is more than two for low latitudes. The largest values of the ratio E_B/E_p occur between 20°N-20°S. There are secondary maxima near the poles which occupy very small surface area and they can be ignored.

We have noted, but we have not explained, that although the SST anomaly was imposed only between the latitudes 0-30°N, the effects on circulation are seen in the southern hemispheric tropics also. This could be due to meridionally propagating Rossby waves forced by heating due to SST anomalies, and interhemispheric interactions associated with the fluctuations of Hadley cells. The results for geopotential height at 500 mb (not shown) are very similar to the one shown in Figure 6 except that the peak at the equator is not as high. These results suggest that SST anomalies in the tropics produce large changes in the middle and upper troposphere. Changes in the organization and intensity of deep moist cnvection introduce significant changes in the diabatic heating of the upper troposphere. For suitable structure and intensity of the prevailing motion fields, these effects can be further transmitted to the middle latitudes.

Sensitivity of the tropical circulation to changes in the boundary conditions.

We have carried out several experiments to test the sensitivity of a global general circulation model to changes in the slowly varying boundary conditions of sea-surface temperature, soil moisture and albedo. It is found that SST anomalies in the low latitudes produce significant changes in the low and the middle latitudes. For example, it is found that the warm (cold) SST anomalies in the Arabian Sea increase (decrease) monsoon rainfall over India and adjoining areas (Shukla, 1975). It is also found that a simultaneous occurrence of warm SST anomalies over the north equatorial Atlantic and cold SST anomalies over the south equatorial Atlantic produce severe drought conditions over northeast Brazil (Moura and Shukla, 1981). A warm anomaly in the north and a cold anomaly in the south generates a thermally driven circulation whose descending branch is over northeast Brazil and adjoining oceans. An SST anomaly over equatorial Atlantic also produces significant middle latitude response in the northern hemisphere. There are numerous other observational and modeling studies which have shown that the tropical SST anomalies influence the intensity of Hadley and Walker cells. Statistically significant relationships have been found between the southern oscillation, SST anomalies in the equatorial Pacific and the upper air circulation over Northern Hemispheric middle latitudes. This suggests that the tropical thermal forcings can contribute to the predictability of the middle latitude time averages, which otherwise are less predictable by themselves.

We have also carried out sensitivity studies for two extreme conditions: In one case, the soil is dry (no evapotranspiration), and in the other case, the soil is wet (potential evapotranspiration) over global land surfaces (Shukla and Mintz, 1981). It is found that during northern summer, absence of land-

surface evapotranspiration over most of the hemisphere reduces the monthly mean rainfall by about half. The only exceptions are the monsoonal regions for which reduction in evaporation over land is more than compensated by the increased moisture flux convergence associated with intense heat lows which form due to intense heating of the ground and the overlying air. In the absence of land evaporation most of the solar radiation is utilized to heat the ground directly and the overlying air is heated by sensible heating.

There are also a few observational and numerical studies which have shown that the extent and the depth of the Eurasian snow cover during winter is related to the intensity of the Asiatc monsoon circulation during the following summer (Hahn and Shukla, 1977; Yeh et al. 1981). The actual mechanism is not quite clear but large snow can give rise to large soil moisture which will impede the heating of the ground needed for the onset of the monsoons.

These results collectively suggest that the boundary conditions at the earth's surface may be a useful predictor for the tropical circulation and under favorable conditions they can contribute to the predictability of the middle latitudes.

Part III. Influence of tropical forcing on the circulation of the extra-tropical atmosphere.

(1) It is a fact of observations that the subtropical highs in the North Atlantic and the South Atlantic have the highest monthly mean sea level pressure simultaneously during the month of July. This is rather remarkable because it is contrary to what one would expect from expected phase lag for the seasonal cycle in the two hemispheres. A possible reason for simultaneous intensification of North and South Atlantic highs may be that they are forced by tropical heating which is also maximum during July. This argument can be generalized to include all the subtropical highs between 30°N and 30°S. Figures 9a and 9b show global maps of 16-year (1961-1976) mean sea level pressure for January and July. We have estimated the intensity of five subtropical highs (North and South Atlantic, North and South Pacific, and South Indian Ocean subtropical highs) by measuring the area enclosed by 1020 mb isobar. Figure 10 shows the plots of the intensity of the subtropical highs as measured by the total area covered by the five subtropical highs and rainfall between the latitude belt 30°N and 30°S for January through December. The rainfall data is taken from Jaeger (1976). It is seen that the intensity of the subtropical highs is closely related to the amount of precipitation and therefore the latent heat of condensation in the tropical belt. It is likely that the interannual variability of the subtropical highs may also be related to the interannual variability of the tropical precipitation. However, adequate precipitation data is not available to test this hypothesis. It should be pointed out that stronger subtropical highs would imply stronger trade winds and possibly stronger intertropical convergence; however, its relationship to rainfall would also depend upon the location of the subtropical highs.

(2) Figure 11 shows the latitudinal distribution of the stationary variance of geopotential height at 500 mb as simulated by two versions of the GLAS climate model. The most important difference between the two simulations was the change in evaporation and precipitation in the tropical belt. The evaporation and precipitation in the old GLAS climate model was less than the observed; the evaporation and precipitation in the modified GLAS climate model is more than the old model and comparable to the observations. The change in the stationary variance in the middle latitudes is rather striking. Although precipitation and evaporation in the mid-latitudes in the modified model were not identical to the old model, and therefore all the change cannot be attributed to the tropical heating, it is reasonable to suggest that the tropical heating is one of the important factors to influence the model simulated stationary variance.

(3) There is some observational evidence that persistent deep moist activity over the tropics can influence the middle latitude circulation within a few days. Paegle (1981) has shown an association between strong outflows at 200 mb between equator and 20°S, and increased transient kinetic energy at 30°N during January and February, 1979. Examination of daily cloud pictures and upper level synoptic weather maps leaves one with the impression (J. Winston, personal communication) of strong association between intense tropical convective activity and intensification of subtropical jet stream.

If tropical activity has strong influence on mid-latitude weather fluctuations, and if tropical flow is unpredictable beyond a few days, does this imply that it would also limit the mid-latitude predictability? It is our conjecture that lack of deterministic predictability for synoptic scales in low latitudes does not necesarily imply that the large-scale tropical-extratropical interactions cannot be adequately modelled. It is the quasi-stationary tropical heat

sources which are the main drivers of the tropical-extratropical teleconnections and produce large extratropical response. It is conceiveable that by suitable procedures of assimilating vertical velocity and diabatic heating fields derived from the observations of cloudiness and precipitation, the large-scale tropical heat sources can be reasonably defined. It is also conceivable that their effects can be accounted for by prescribing them for a few days.

(4) Kalnay-Rivas and Halem (personal communication) have carried out several forecast experiments during FGGE SOPI with the GLAS forecast model. For four of the cases they inserted the observed FGGE data every six hours during the forecast between 20°S and 20°N. This was intended to simulate a perfect forecast in the tropics. They compared the skill of the forecasts over North America for the normal forecasts and the forecasts with tropical FGGE data inserted during the forecasts. In three out of four forecasts, insertion of tropical data had little effect on the forecast skill over North America; however, in one of the four cases there was substantial improvement in the forecast for North America after the first three days of integration. Cloud pictures showed the presence of an intense tropical flux originating in the equatorial Western Pacific and penetrating deep into the mid-latitudes reaching the west coast of America.

Although more observational and numerical studies are needed to establish the nature of tropical-mid-latitude interaction at such 'fast' time scales, preliminary results suggest that tropical phenomena, in some situations, may be important even for short range NWP in middle latitudes.

(5) There is yet no quantitative assessment of the relative roles of data assimilation and initialization procedures, parameterization of moist convective heating, and poor definition of initial state for rapid degradation of tropical forecasts. If moist convection parameterization is not realistic, it quickly

produces unrealistic flow which in turn leads to still more unrealistic moist convective heating. This fast feedback between the motion field and the moist convective heating may be one of the most important limiting factors for tropical predictability. Large sensitivity of tropical forecasts to changes in the initial moisture field support this point. It is therefore conceivable that prescribing the condensation heating may be less damaging than explicitly calculating it. This could be true even for middle and high latitudes.

Conclusions:

Classical predictability studies using a general circulation model show that for short- and medium-range the tropical atmosphere is less predictable than the middle latitudes. This is primarily because of the following reasons: 1) Tropical areas have less data and therefore more uncertainty in the initial conditions. The error of observations is comparable to the changes to be predicted. 2) Most of the day-to-day fluctuations are due to condensation driven instabilities which grow rapidly. The initialization and assimilation techniques do not take into account the role of diabatic forcing for tropical disturbances and it is difficult to parameterize the physical processes of moist convection, boundary layer and cloud-radiation interaction. 3) The standard deviation of day-to-day fluctuations is relatively small because the amplitudes of the tropical disturbances equilibrate rapidly. It takes only a few days for the initial error to grow to be comparable to the standard deviation of daily fluctuations.

On the other hand, the time averages (monthly and seasonal means) for the tropics have more potential predictability. This is because they are largely determined by fluctuations in the slowly varying boundary conditions of sea surface temperature and soil moisture. Under favorable conditions they can contribute to the predictability of middle latitudes also.

Evidence is beginning to emerge that tropical heat sources can also influence the middle latitude circulation within a few days. If the tropical atmosphere were intrinsically unpredictable for the short and medium ranges, its influence on the middle latitudes will also be unpredictable. We conjecture that it is the quasi-steady component of the tropical heat source which affects the middle latitude circulation and therefore it should be possible, in principle, to prescribe it for a few days from the observations. This may require special techniques of initialization and assimilation of tropical data of cloudiness (vertical velocity) and rainfall (heating).

Acknowledgements:

This article was prepared in response to an invitation from Dr. D. B. Shaw to participate in a workshop at the European Centre for Medium Range Weather Forecasts. Prof. R. S. Lindzen, Drs. R. Atlas and D. Straus made valuable suggestions on the first draft of the paper. Prof. J. Paegle and Dr. E. Kalnay kindly communicated their unpublished results on the influence of tropics on the mid-latitudes. Excellent typing and drafting was done by Miss Debbie Boyer and Miss Laura Rumburg.

REFERENCES

Charney, J. G., R. G. Fleagle, V. E. Lally, H. Riehl, and D. Q. Wark, 1966: The feasibility of a global observation and analysis experiment. Bull. Amer. Meteor. Soc., 47, 200-220.

Charney, J. G., W. J. Quirk, S. Chow, and J. Kornfield, 1977: A comparative study of the effects of albedo change on drought in semi-arid regions. J. Atmos. Sci., 34, 1366.

Charney, J. G., and J. Shukla, 1981: Predictability of monsoons. Monsoon Dynamics, Cambridge University Press, Editors: Sir James Lighthill and R. P. Pearce.

Godbole, R. V., and J. Shukla, 1981: Global analysis of January and July sea level pressure. NASA Tech. Memo. 82097.

Hahn, D., and J. Shukla, 1976: An apparent relationship between Eurasian snow cover and Indian monsoon rainfall. J. Atmos. Sci., 33, 2461-2463.

Halem, M., J. Shukla, Y. Mintz, M. L. Wu, R. Godbole, G. Herman, and Y. Sud, 1979: Climate comparisons of a winter and summer numerical simulation with the GLAS general circulation model. GARP Publication Series, 22, 207-253.

Jaeger, L., 1976: Montaskarten des Niederschlages fur die ganze Erde. Berichte Dentscher Wetterd. Nr. 139, Ottenbach.

Lorenz, E. N., 1969: The predictability of a flow which possesses many scales of motion. Tellus, 21, 289-306.

Moura, D. A., and J. Shukla, 1981: On the dynamics of droughts in northeast Brazil: observations, theory and numerical experiments with a general circulation model. (submitted to J. Atmos. Sci.)

Paegle, J. N., 1981: Short term influence radius of monsoonal overturnings. Conference on early results of FGGE/MONEX, Jan., 1981, Tallahassee, Florida.

Shukla, J., 1975: Effect of Arabian sea-surface anomaly on Indian summer monsoon: A numerical experiment with GFDL model. J. Atmos. Sci., 32, 503-511.

Shukla, J., 1978: CISK-barotropic-baroclinic instability. J. Atmos. Sci., 35, 495-508.

Shukla, J., and Y. Mintz, 1981: The influence of land-surface evapotranspiration on the earth's climate. (in preparation)

Smagorinsky, J., 1969: Problems and promises of deterministic extended range forecasting. Bull. Amer. Meteor. Soc., 50, 286-311.

Stevens, D. E., R. S. Lindzen, and L. J. Shapiro, 1977: A new model of tropical waves incorporating momentum mixing by cumulus convection. Dyn. Atm. Oceans, 1, 365-425.

Straus, D. M., and M. Halem, 1981: A stochastic-dynamical approach to the study of the natural variability of the climate. Mon. Wea. Rev., 109, 407-421.

Yeh, T. C., X. C. Chen, and C. B. Fu, 1981: The feedback process of large scale precipitation on the variation of atmospheric circulation and climate, the air-land interaction. (pre-published manuscript.)

Figures

Fig. 1a. Root mean square error between four summer model runs as a function of time for zonal velocity (m/s) at 175 mb. Solid line, dashed line and dotted line refer to an average over 10° latitude belt centered at 6°N, 30°N and 58°N respectively.

Fig. 1b. Same as Fig. 1a but for sea level pressure (mb).

Fig. 2a. Zonally averaged values of the ratio of root mean square error between four summer model runs and standard deviation of daily values for the same four runs for zonal velocity at 175 mb. Curve labeled as DAY 1,2,3,7 refer to the ratio at the end of one, two, three and seven days.

Fig. 2b. Same as Fig. 2a but for zonal velocity at 835 mb.

Fig. 2c. Same as Fig. 2a but for sea level pressure.

Fig. 3. Doubling time (days) for the initial error among the four predictability runs of sea level pressure (solid line), zonal velocity at 835 mb (dashed line) and zonal velocity at 175 mb (dotted line).

Fig. 4a. Root mean square as a function of time between a summer control and a predictability run for sea level pressure (mb). Solid line, dashed line and dotted line refer to an average over 10° latitude belt centered at 6°N, 30°N and 58°N respectively.

Fig. 4b. Same as Fig. 4a but for zonal velocity (m/s) at 500 mb.

Fig. 4c. Same as Fig. 4a but for meridional velocity (m/s) at 500 mb.

Fig. 4d. Same as Fig. 4a but for temperature (°C) at 500 mb.

Fig. 5a. Root mean square error between four winter model runs as a function of latitude and time (day) for geopotential height at 500 mb.

Fig. 5b. Zonally averaged values of the ratio of root mean square between nine pairs of winter model runs and standard deviation of daily values for geopotential height at 500 mb.

Fig. 6a. Difference between the climatological sea surface temperature used for the control run and observed sea surface temperature during July 1972 between equator and 30°N.

Fig. 6b. Same as Fig. 6a but for July 1973.

Fig. 6c. Same as Fig. 6a but for July 1974.

Fig. 7. Zonally averaged standard deviation among monthly mean (July) sea level pressure (mb) for 10 years of observations (σ_o, thin solid line) dashed line) and four model runs with identical boundary conditions (σ_p, thin dotted line). Thick solid line and thick dashed line show the ratio σ_o/σ_p and σ_o/σ_B respectively.

Fig. 8. Zonally averaged standard deviation for predictability runs (thin solid line), boundary forced runs (dashed line) and the ratio of boundary forced and predictability runs (thick solid line) for geopotential height at 300 mb.

Fig. 9a. Sixteen year (1961-76) mean sea level pressure (-1000 mb) for January.

Fig. 9b. Sixteen year (1961-76) mean sea level pressure (-1000 mb) for July.

Fig. 10. Variation of monthly mean rainfall (mm) averaged between 30°N and 30°S (from Jaeger, 1976), and intensity of subtropical highs measured by number of (4° lat. x 5° long.) grid points for which sea level pressure is greater than 1020 mb (from Godbole and Shukla, 1981).

Fig. 11. Stationary variance of January mean geopotential height at 500 mb simulated by two versions of the GLAS climate model, and observations.

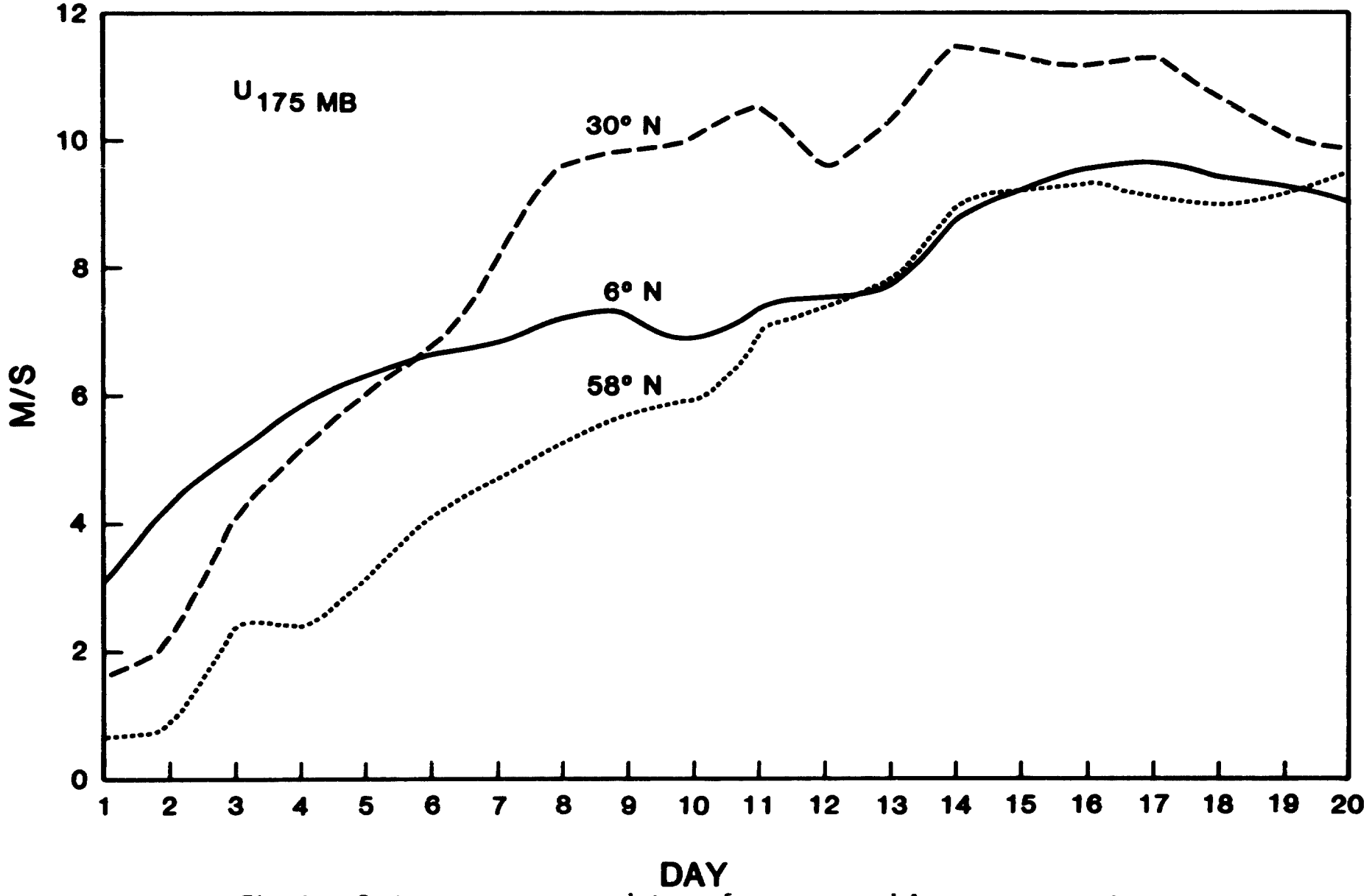

Fig. 1a. Root mean square error between four summer model runs as a function of time for zonal velocity (m/s) at 175 mb. Solid line, dashed line and dotted line refer to an average over 10° latitude belt centered at 6°N, 30°N and 58°N respectively.

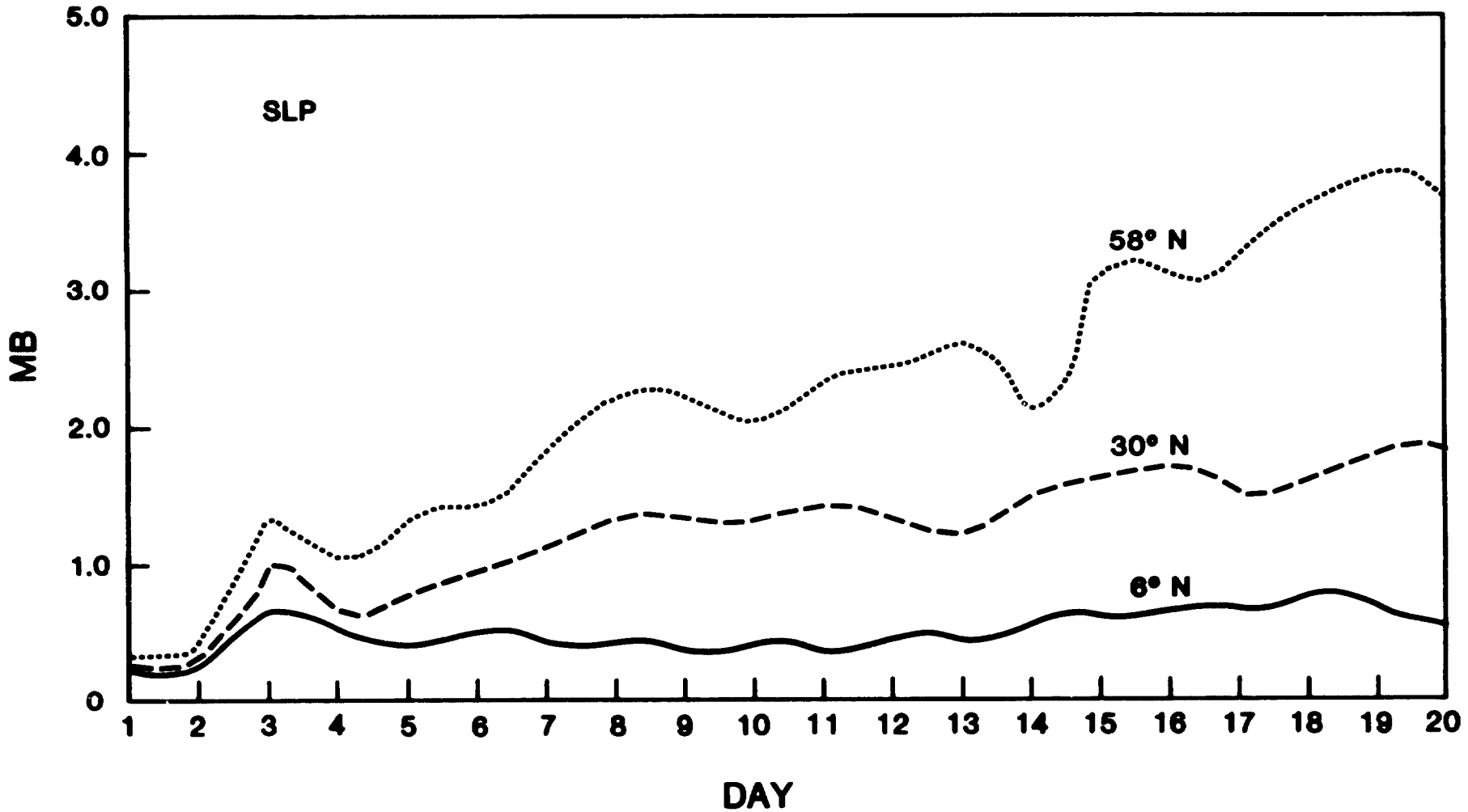

Fig. 1b. Same as Fig. 1a but for sea level pressure (mb).

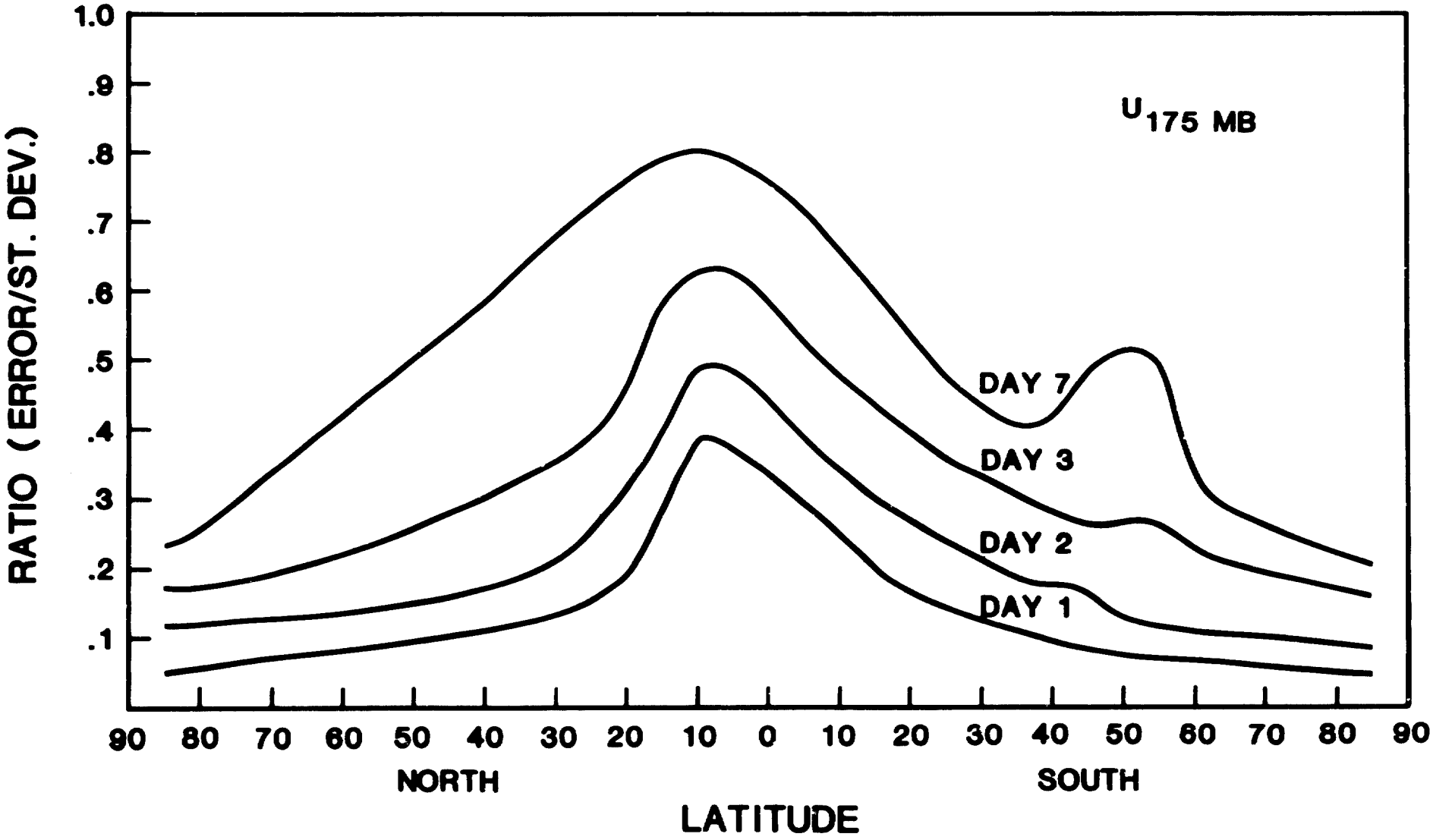

Fig. 2a. Zonally averaged values of the ratio of root mean square error between four summer model runs and standard deviation of daily values for the same four runs for zonal velocity at 175 mb. Curve labeled as DAY 1,2,3,7 refer to the ratio at the end of one, two, three and seven days.

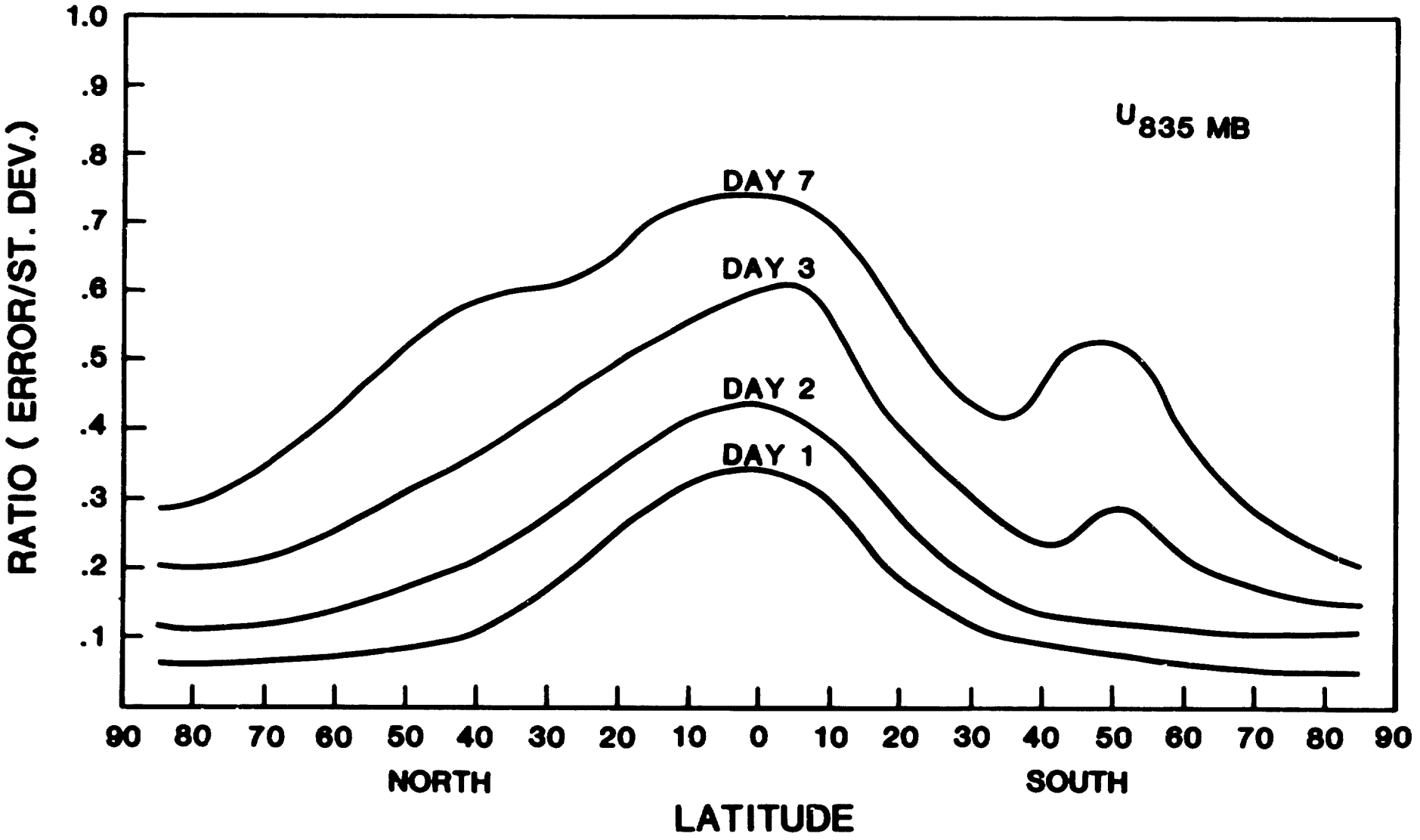

Fig. 2b. Same as Fig. 2a but for zonal velocity at 835 mb.

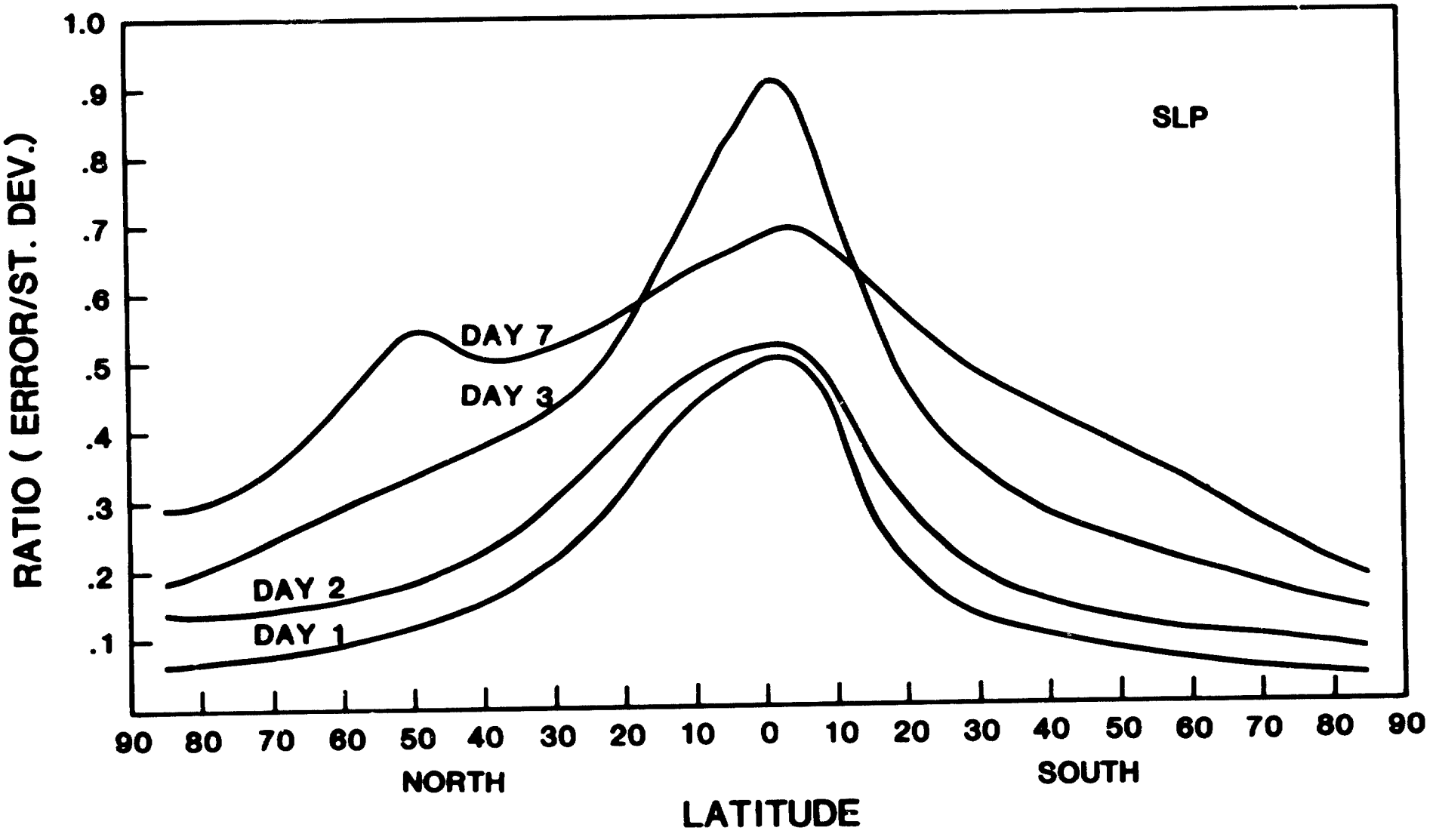

Fig. 2c. Same as Fig. 2a but for sea level pressure.

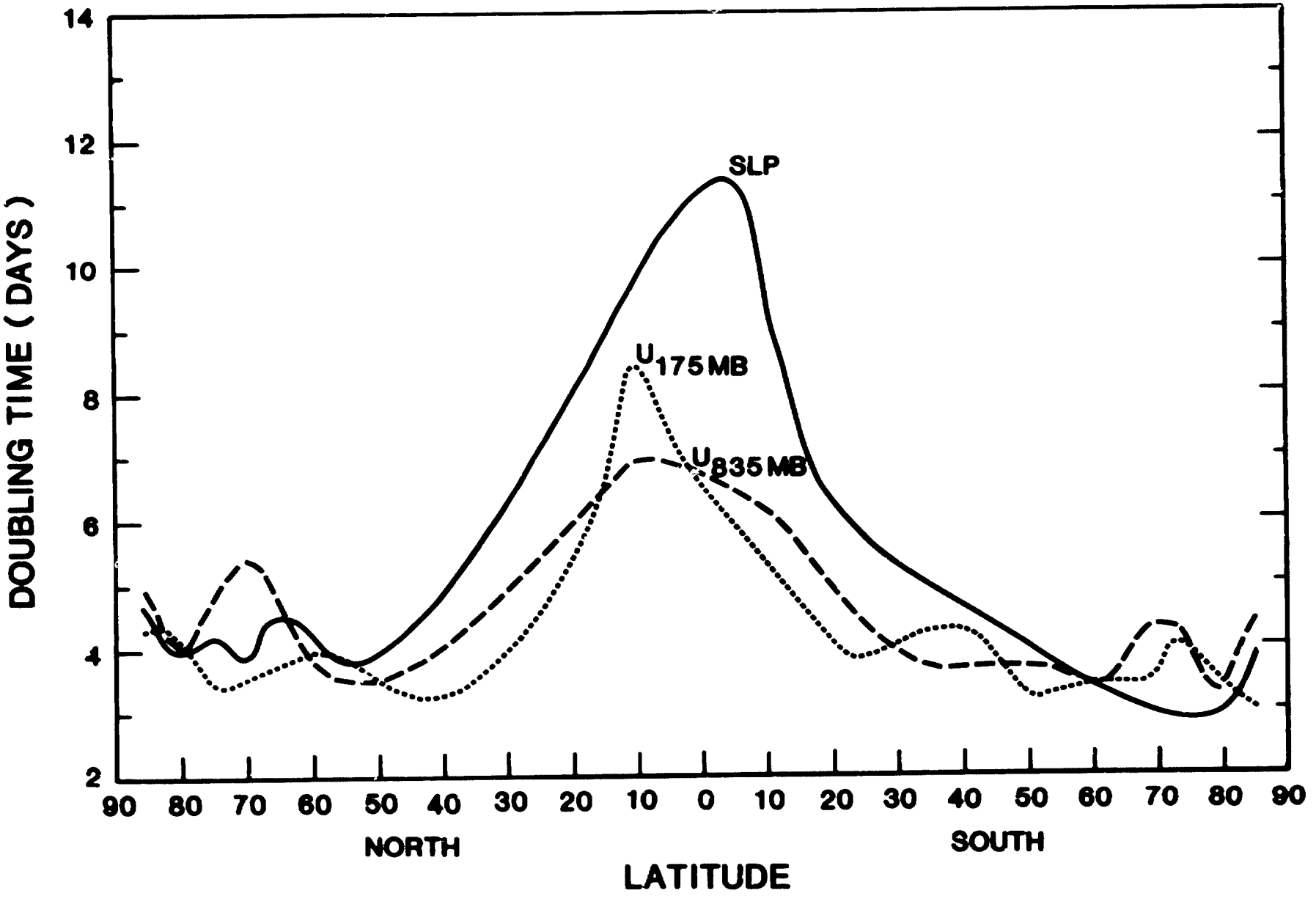

Fig. 3. Doubling time (days) for the initial error among the four predictability runs of sea level pressure (solid line), zonal velocity at 835 mb (dashed line) and zonal velocity at 175 mb (dotted line).

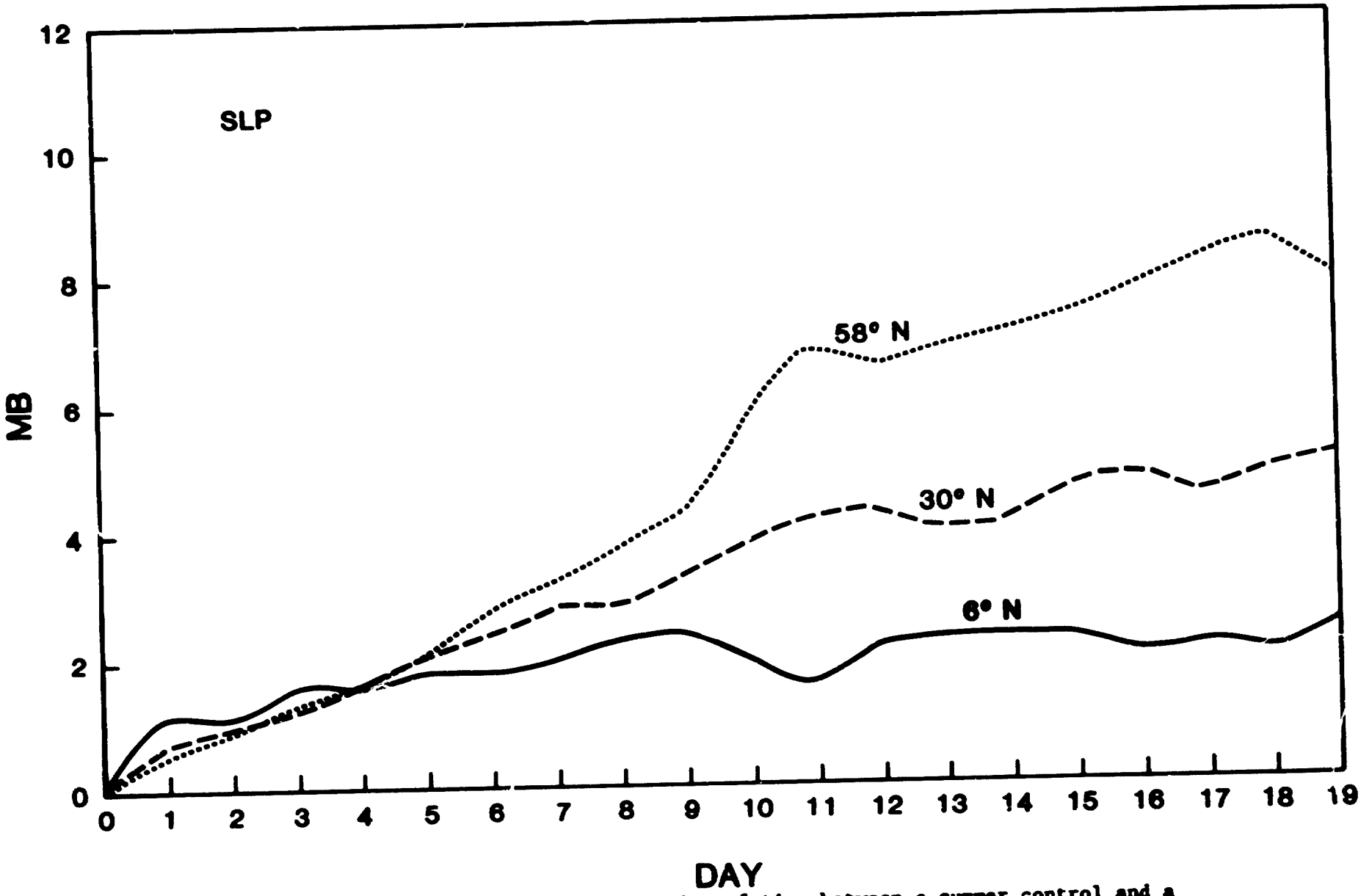

Fig. 4a. Root mean square as a function of time between a summer control and a predictability run for sea level pressure (mb). Solid line, dashed line and dotted line refer to an average over 10° latitude belt centered at 6°N, 30°N and 58°N respectively.

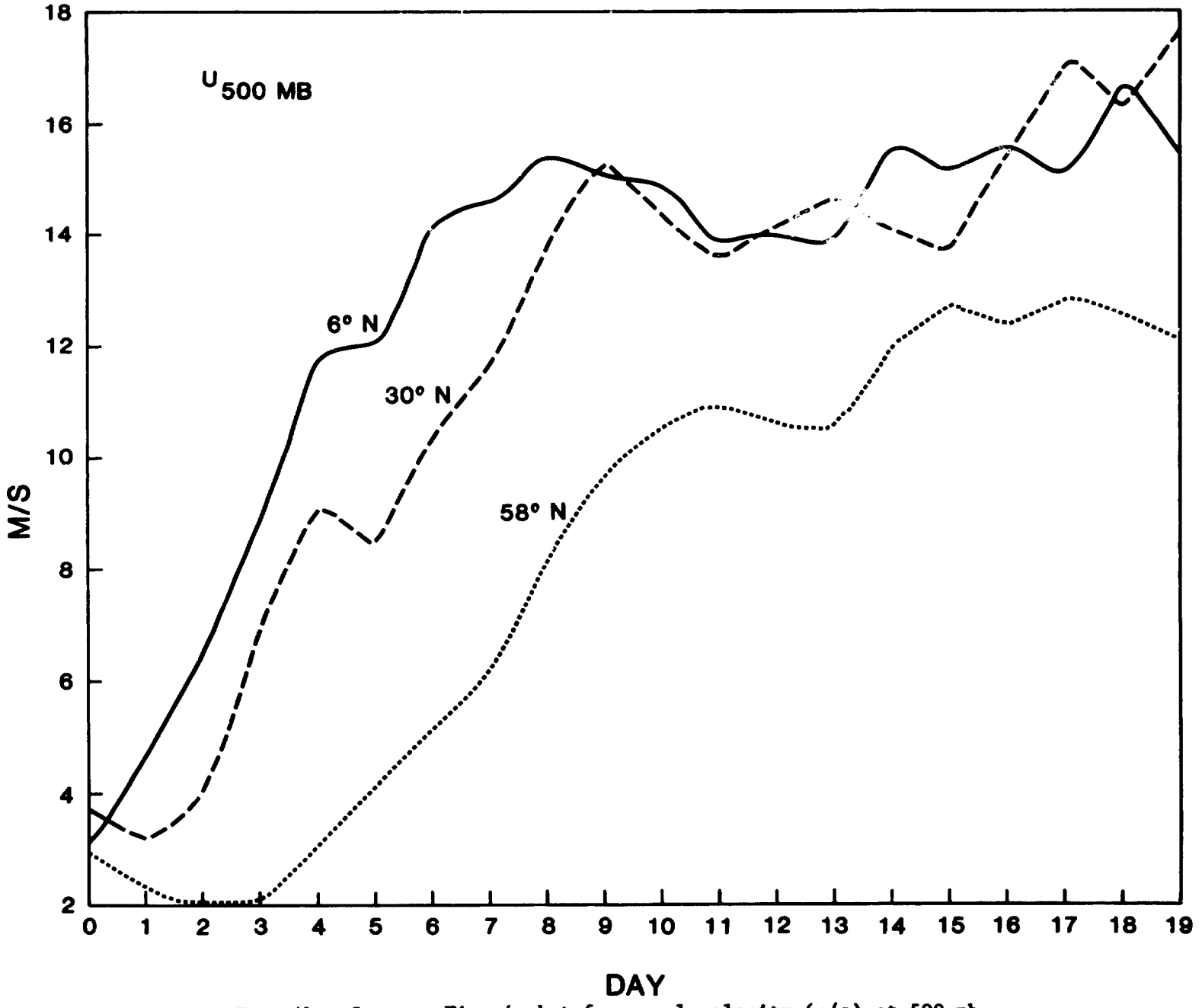

Fig. 4b. Same as Fig. 4a but for zonal velocity (m/s) at 500 mb.

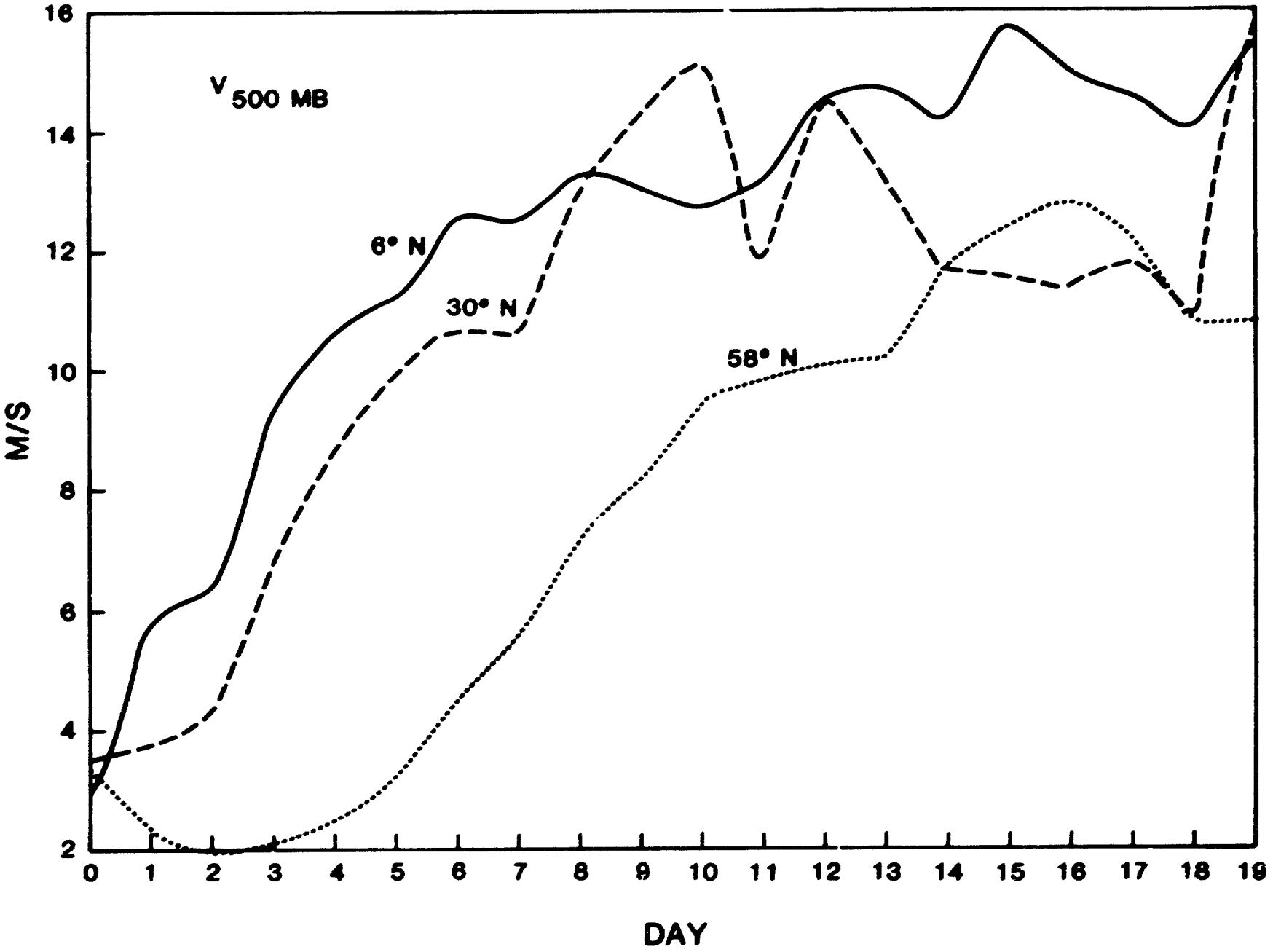

Fig. 4c. Same as Fig. 4a but for meridional velocity (m/s) at 500 mb.

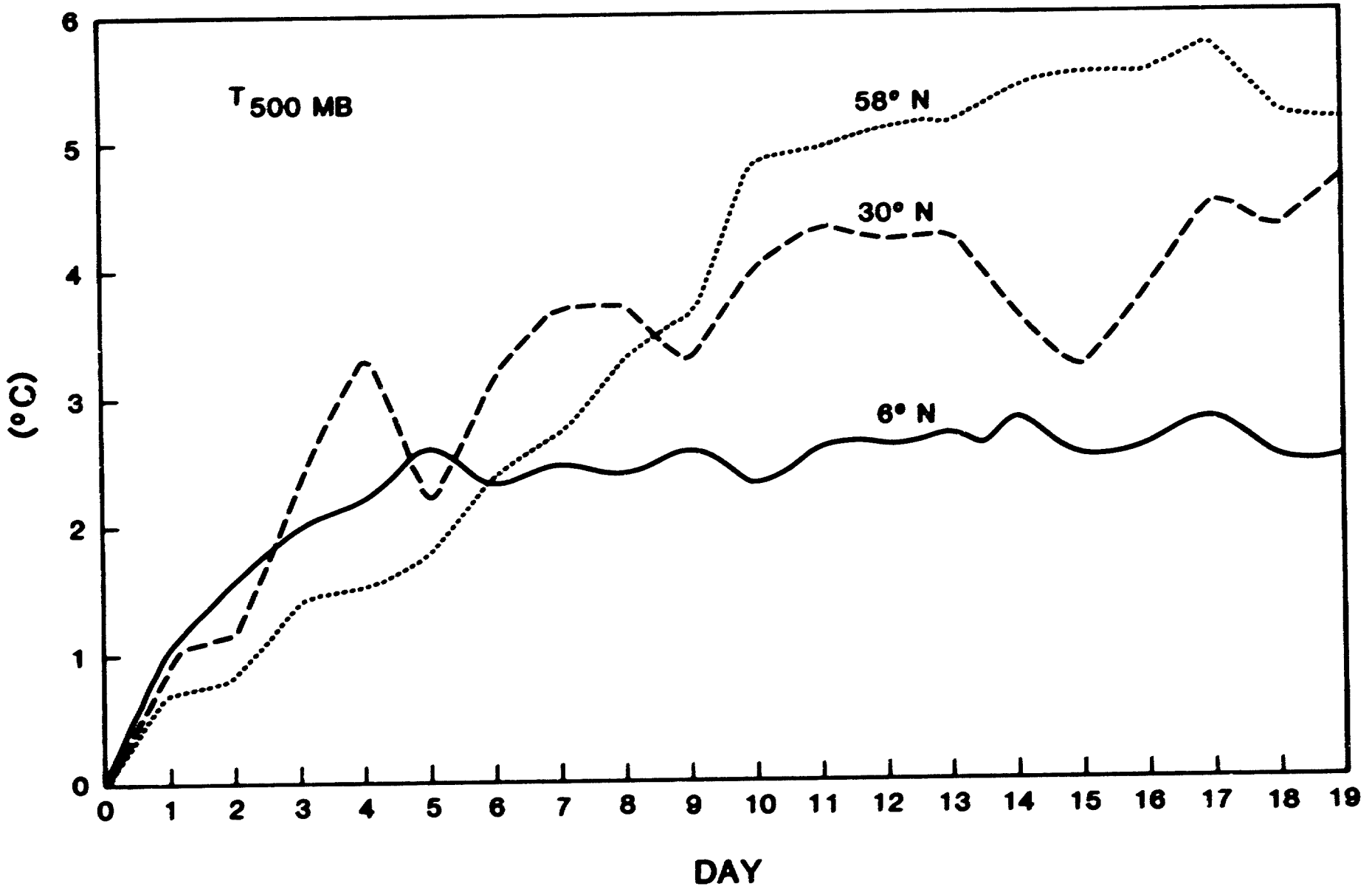

Fig. 4d. Same as Fig. 4a but for temperature (°C) at 500 mb.

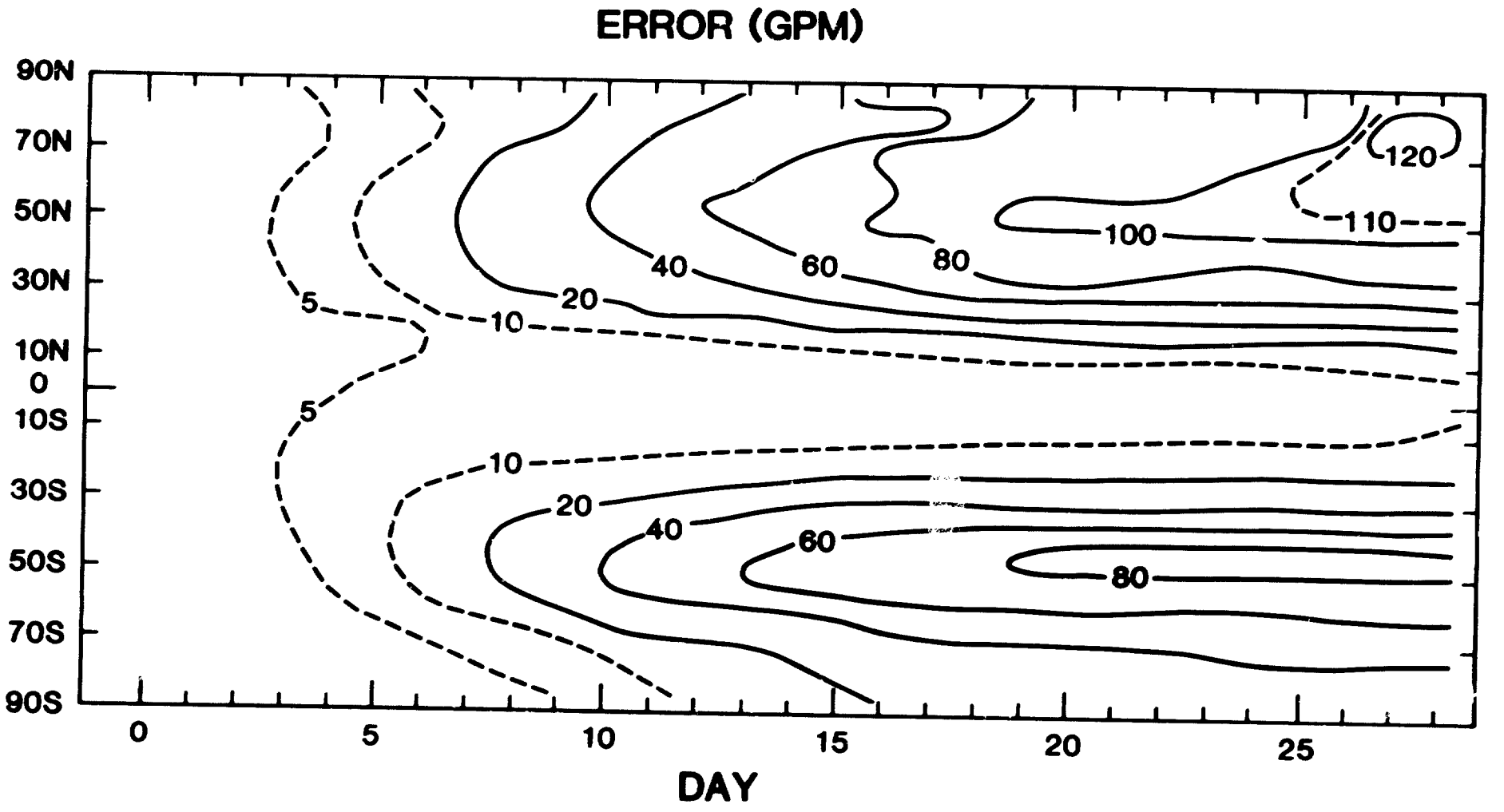

Fig. 5a. Root mean square error between four winter model runs as a function of latitude and time (day) for geopotential height at 500 mb.

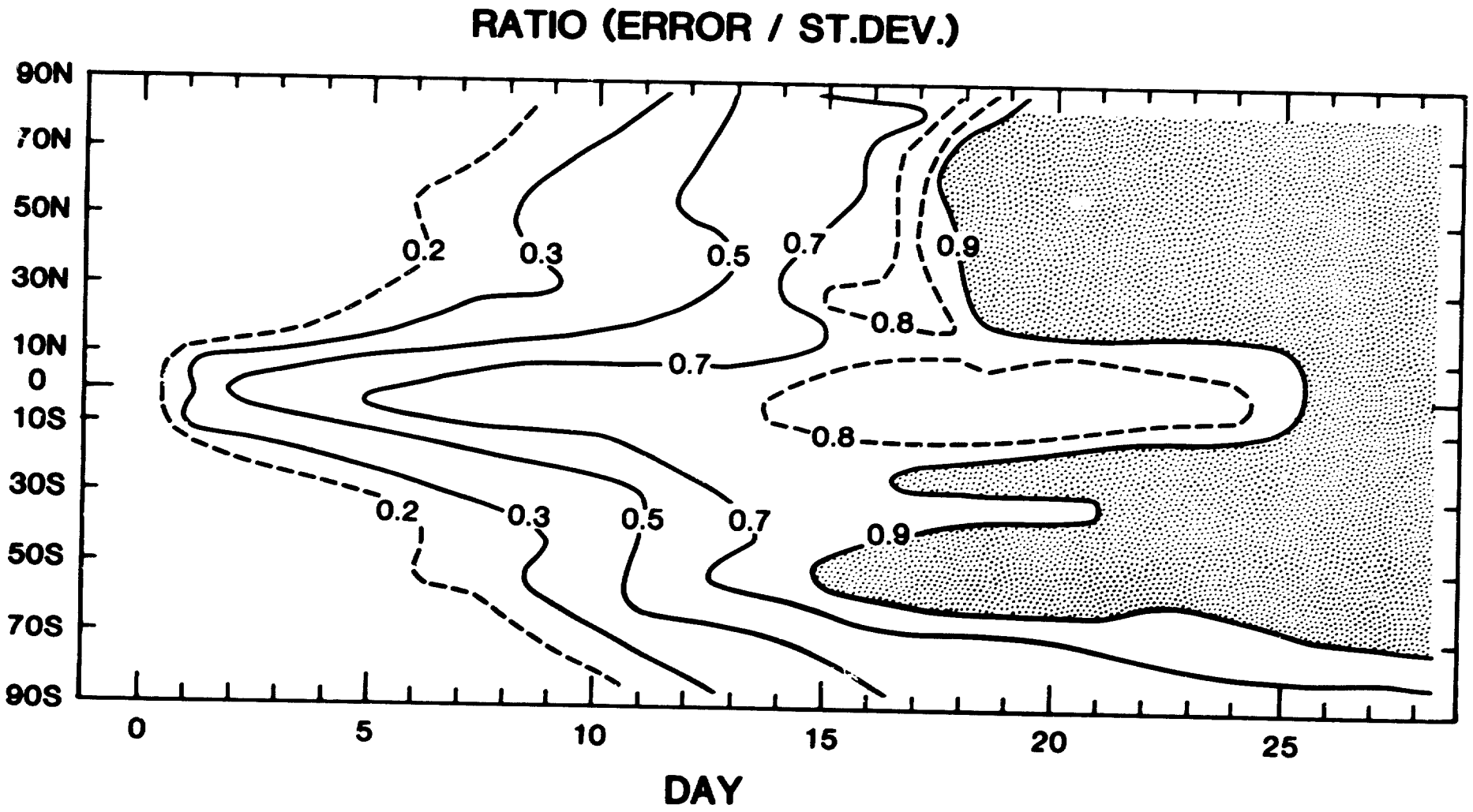

Fig. 5b. Zonally averaged values of the ratio of root mean square between nine pairs of winter model runs and standard deviation of daily values for geopotential height at 500 mb.

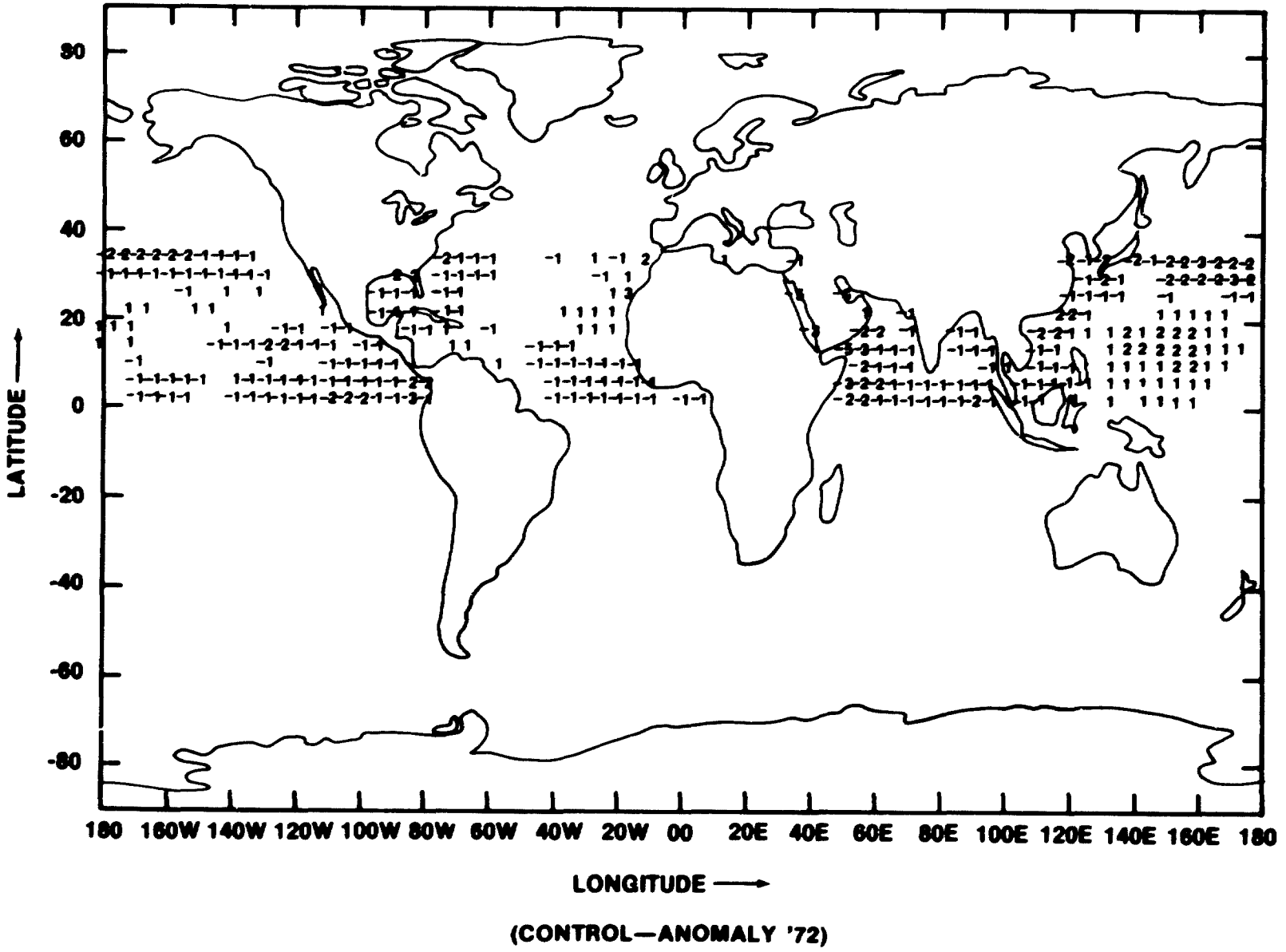

Fig. 6a. Difference between the climatological sea surface temperature used for the control run and observed sea surface temperature during July 1972 between equator and 30°N.

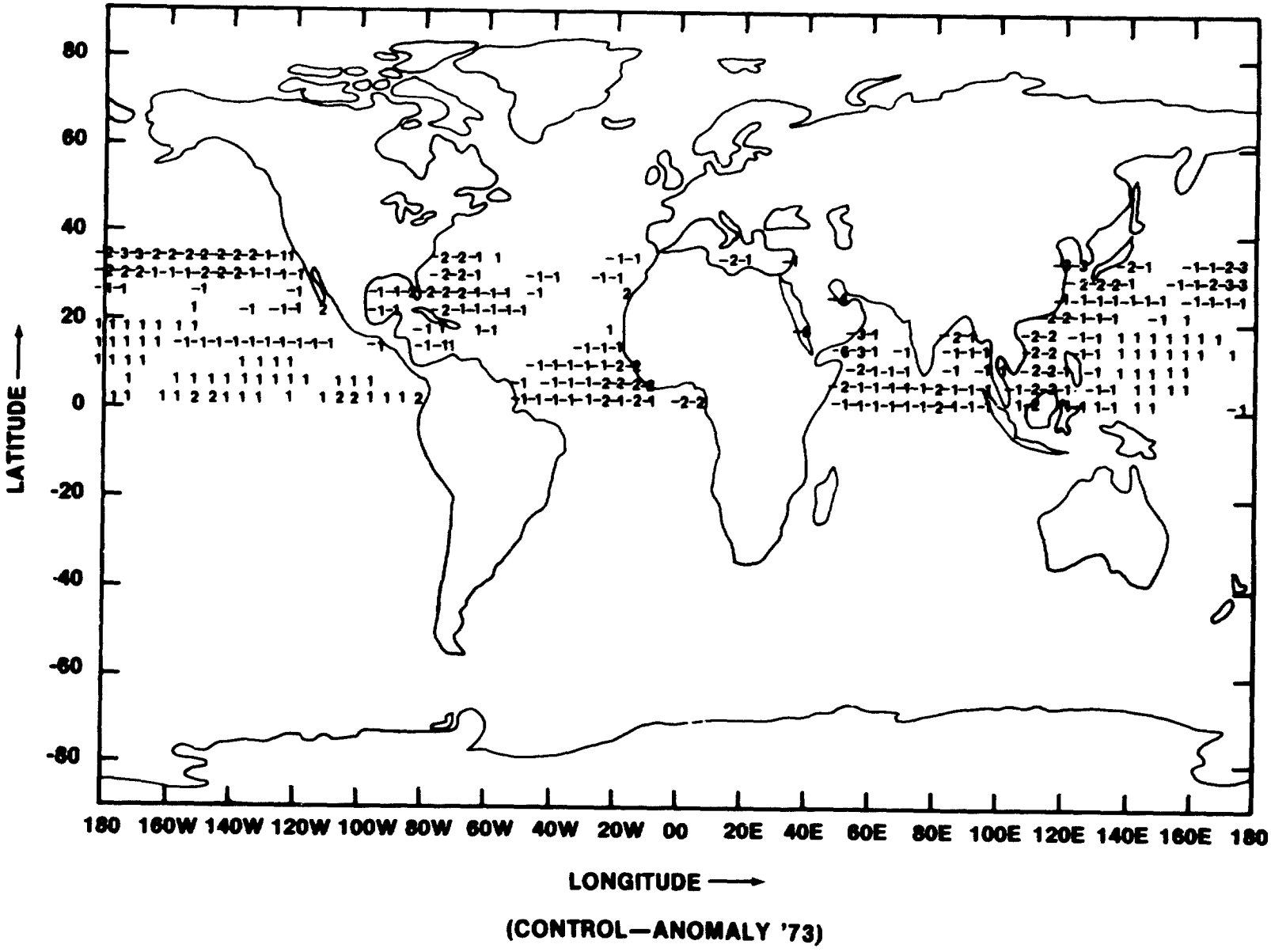

Fig. 6b. Same as Fig. 6a but for July 1973.

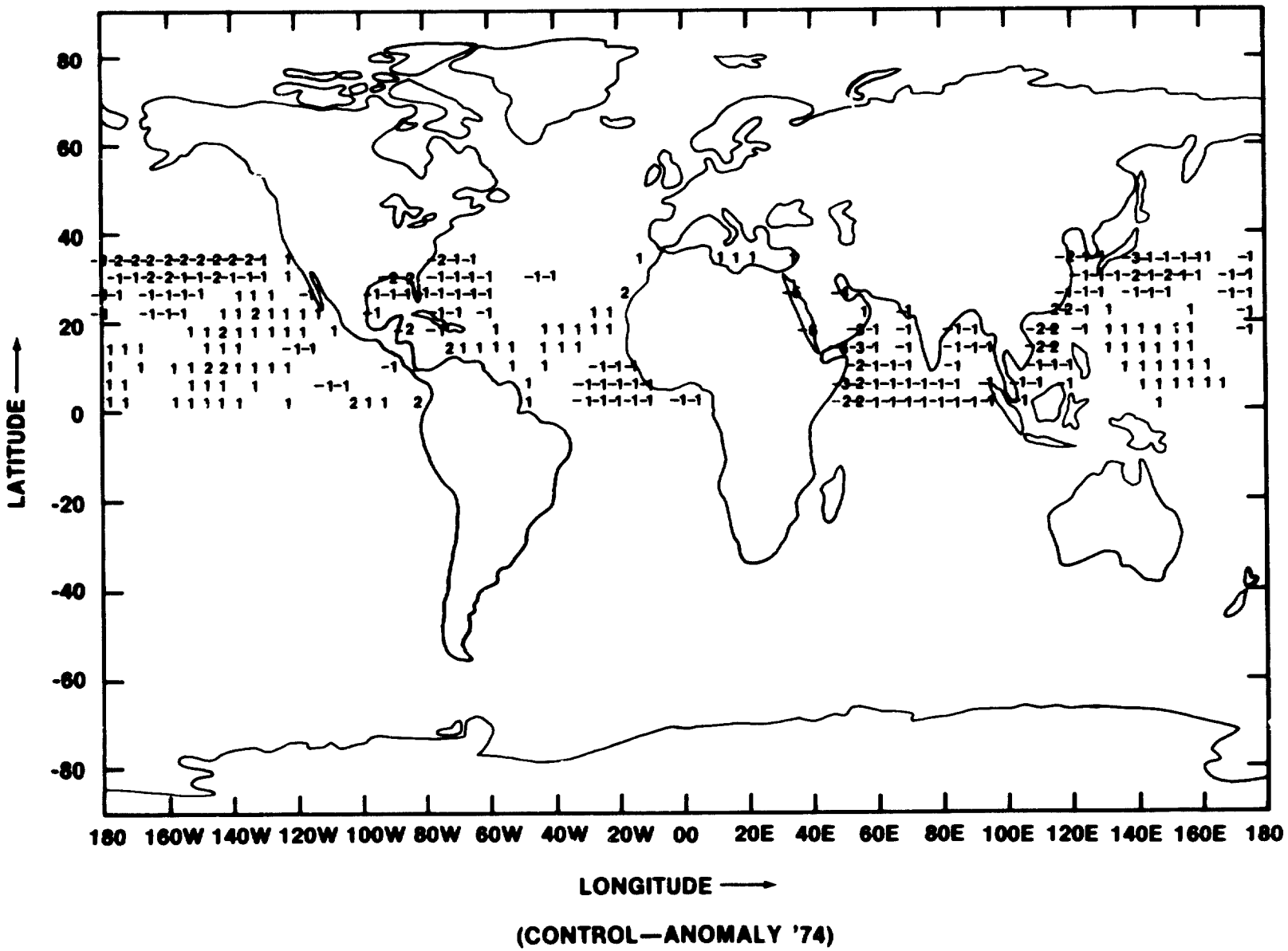

Fig. 6c. Same as Fig. 6a but for July 1974.

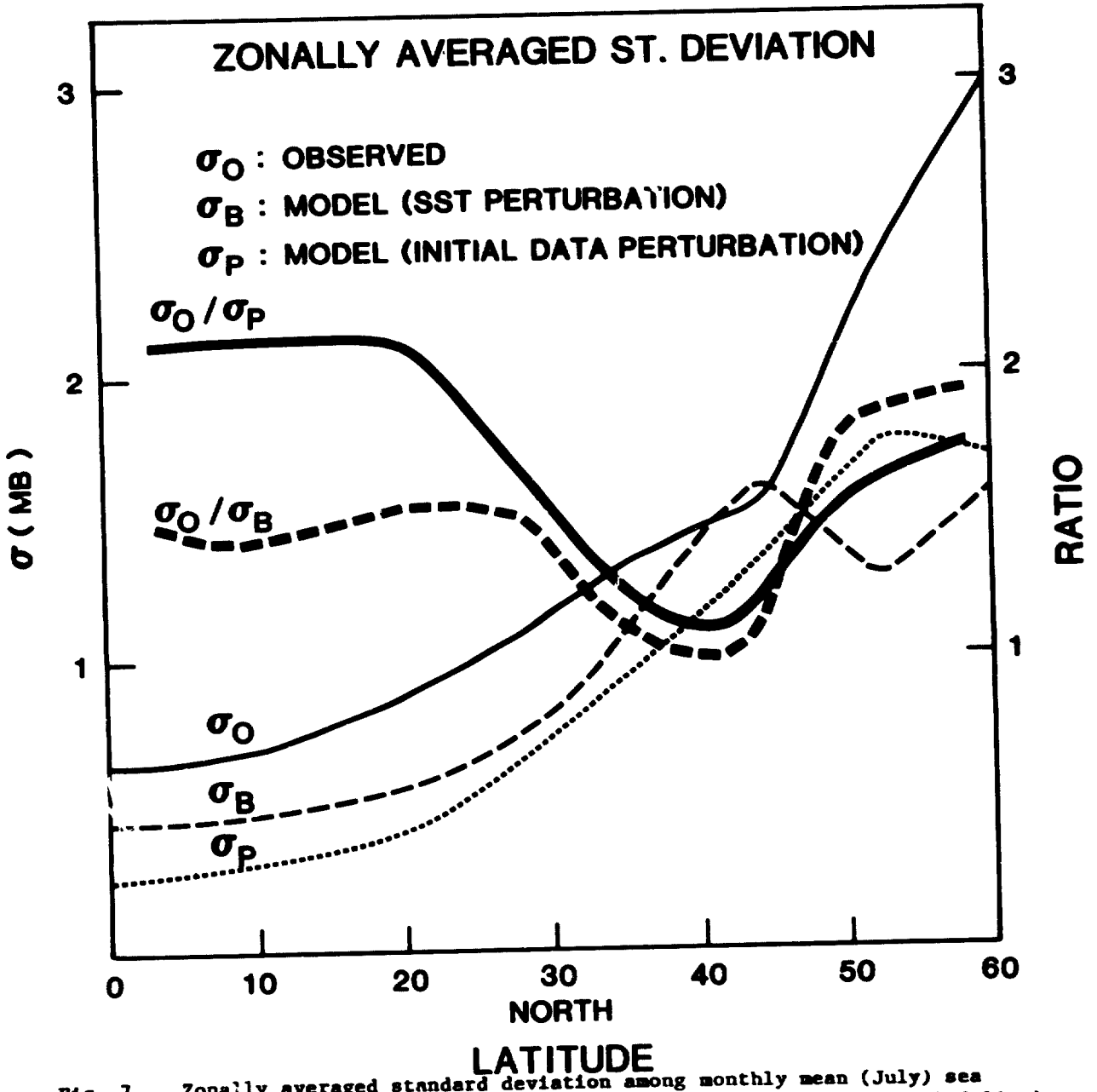

Fig. 7. Zonally averaged standard deviation among monthly mean (July) sea level pressure (mb) for 10 years of observations (σ_o, thin solid line) dashed line) and four model runs with identical boundary conditions (σ_p, thin dotted line). Thick solid line and thick dashed line show the ratio σ_o/σ_p and σ_o/σ_B respectively.

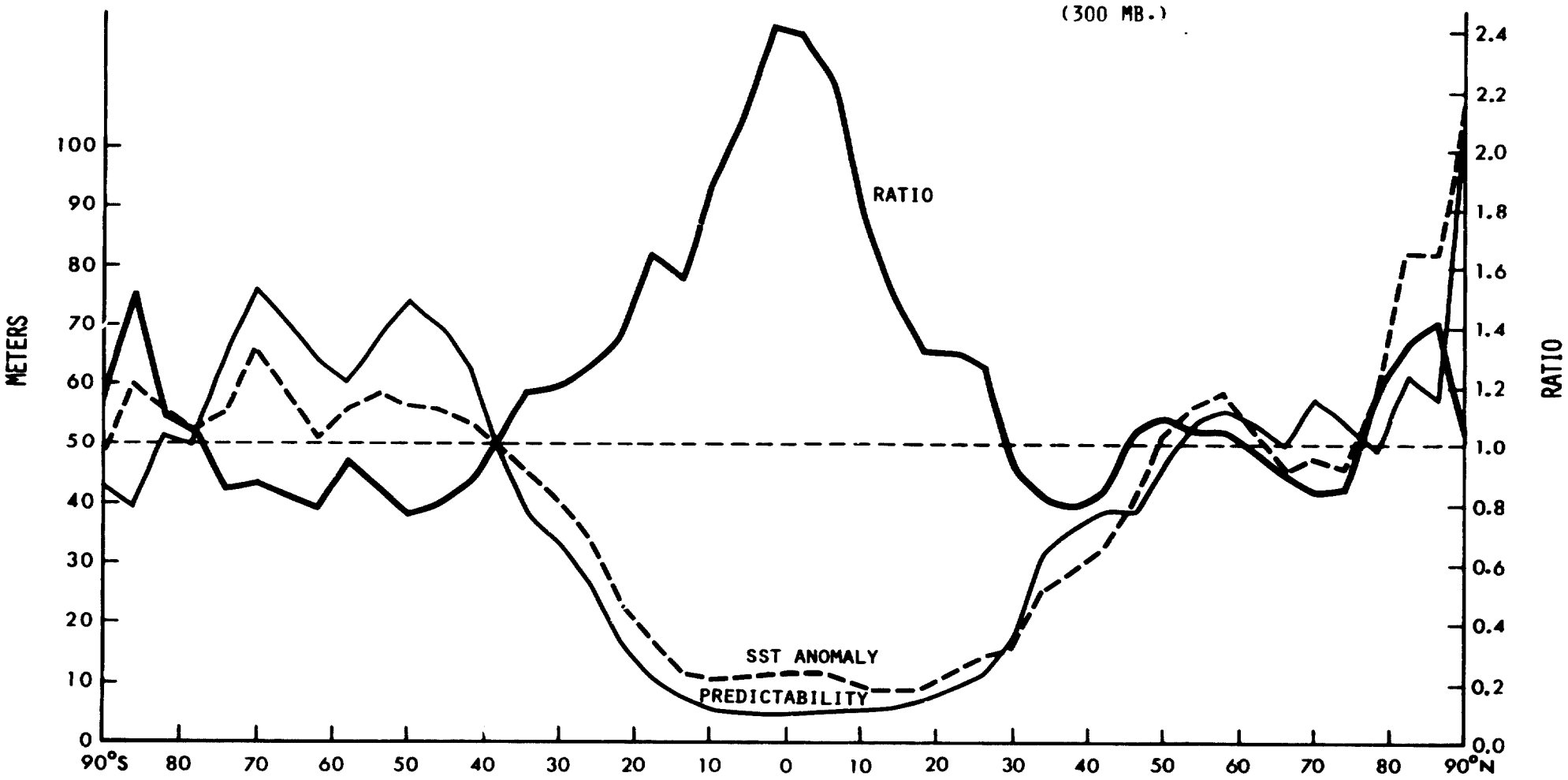

Fig. 8. Zonally averaged standard deviation for predictability runs (thin solid line), boundary forced runs (dashed line) and the ratio of boundary forced and predictability runs (thick solid line) for geopotential height at 300 mb.

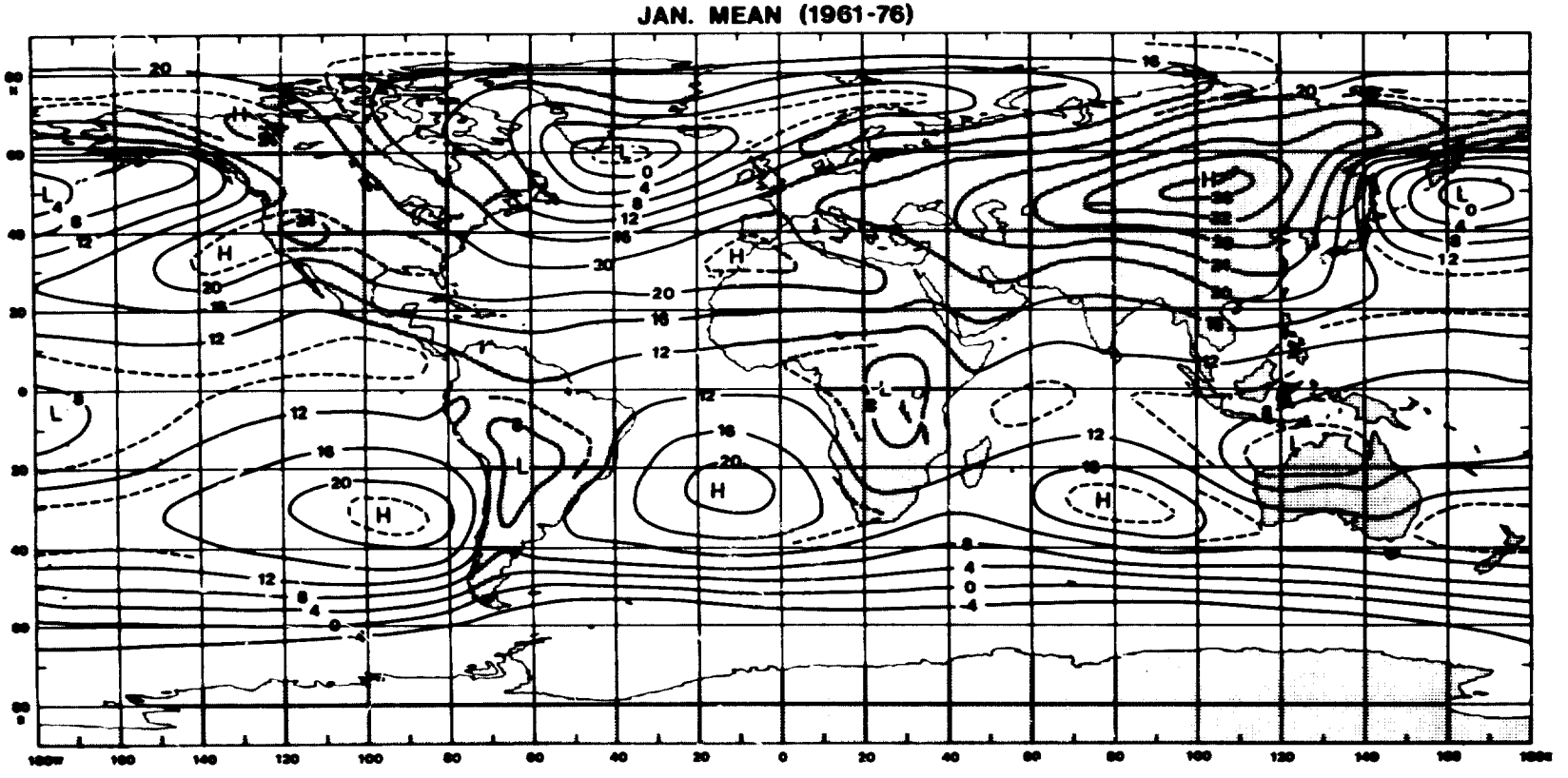

Fig. 9a. Sixteen year (1961-76) mean sea level pressure (-1000 mb) for January.

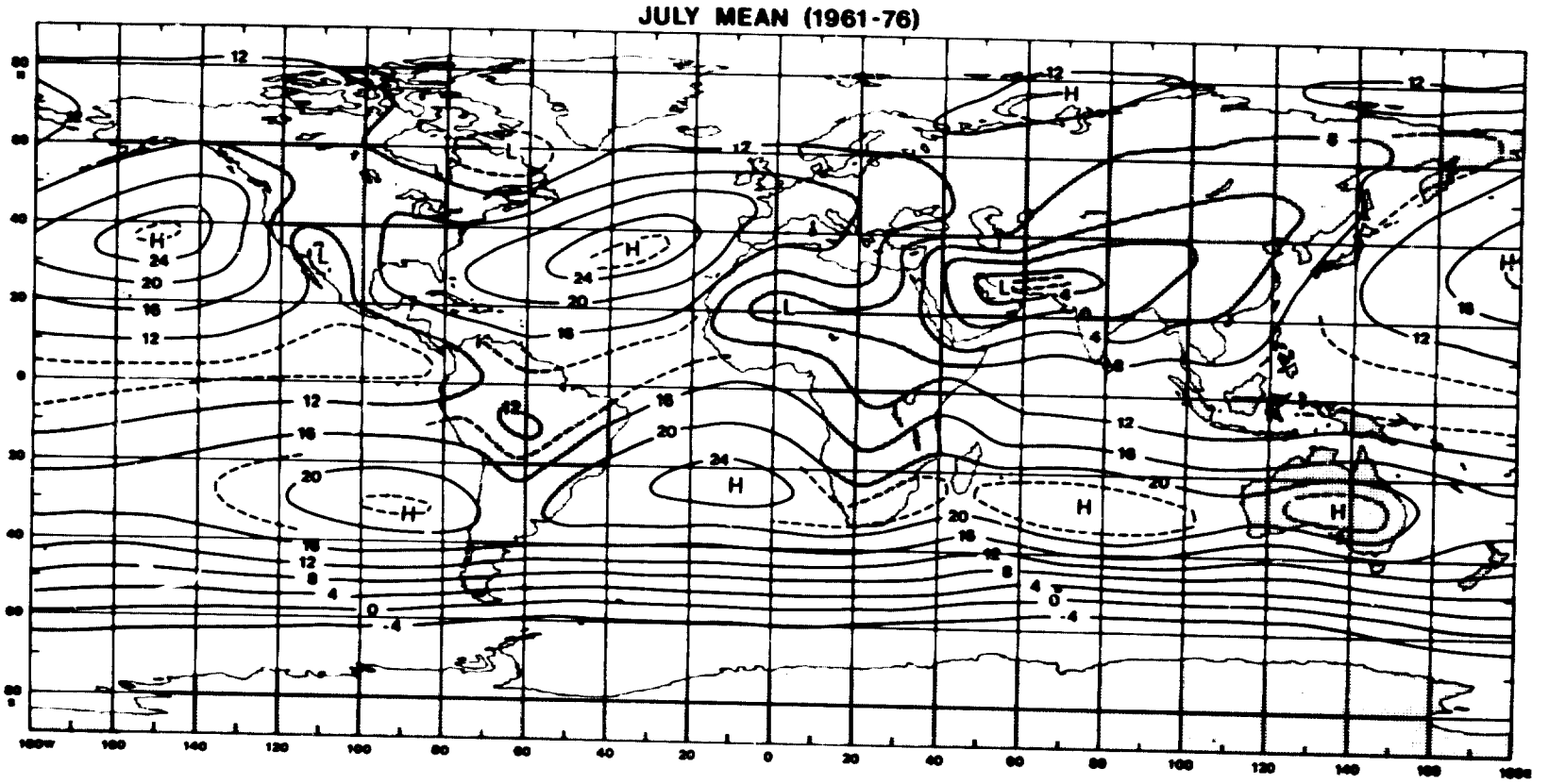

Fig. 9b. Sixteen year (1961-76) mean sea level pressure (-1000 mb) for July.

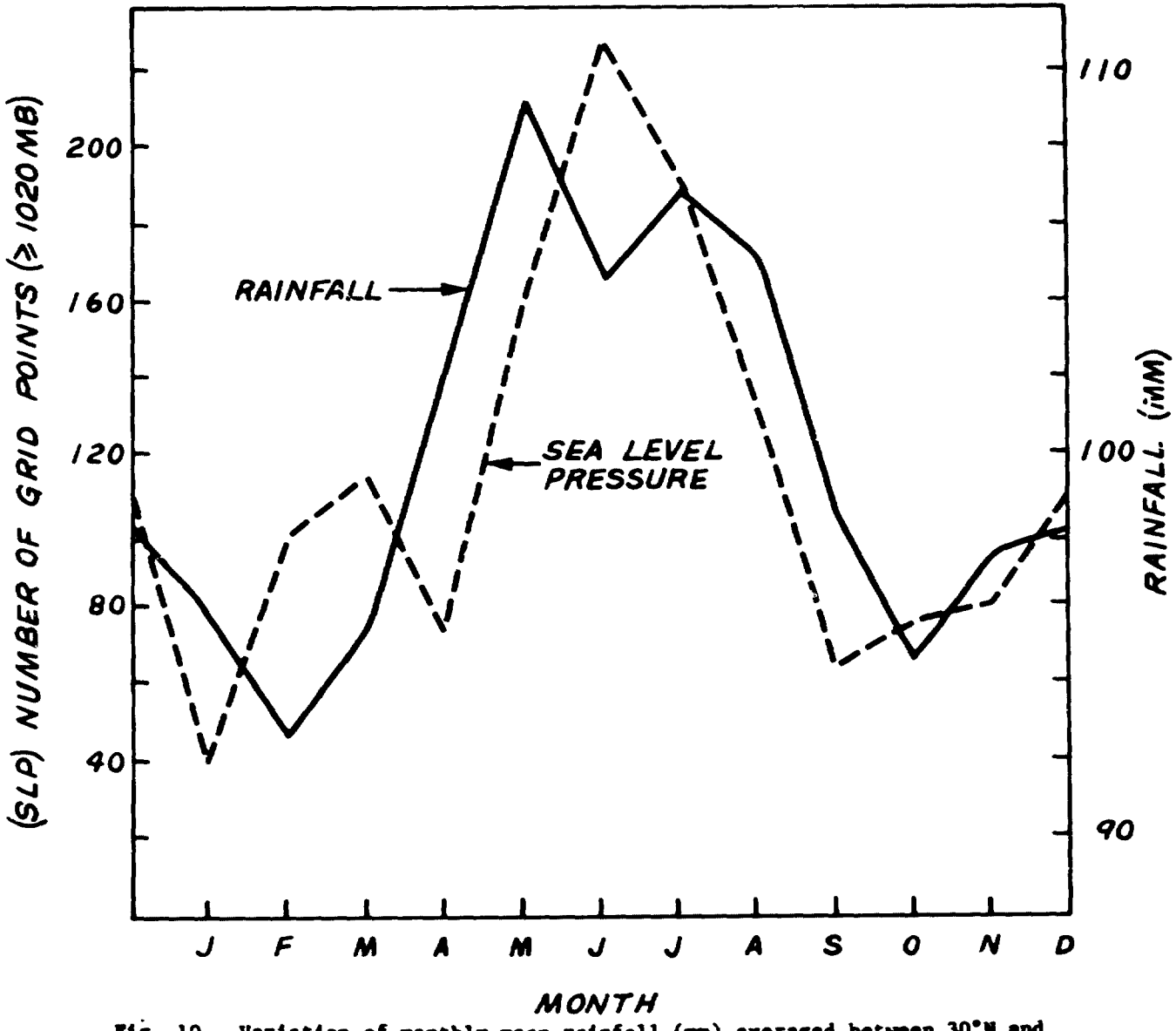

Fig. 10. Variation of monthly mean rainfall (mm) averaged between 30°N and 30°S (from Jaeger, 1976), and intensity of subtropical highs measured by number of (4° lat. x 5° long.) grid points for which sea level pressure is greater than 1020 mb (from Godbole and Shukla, 1981).

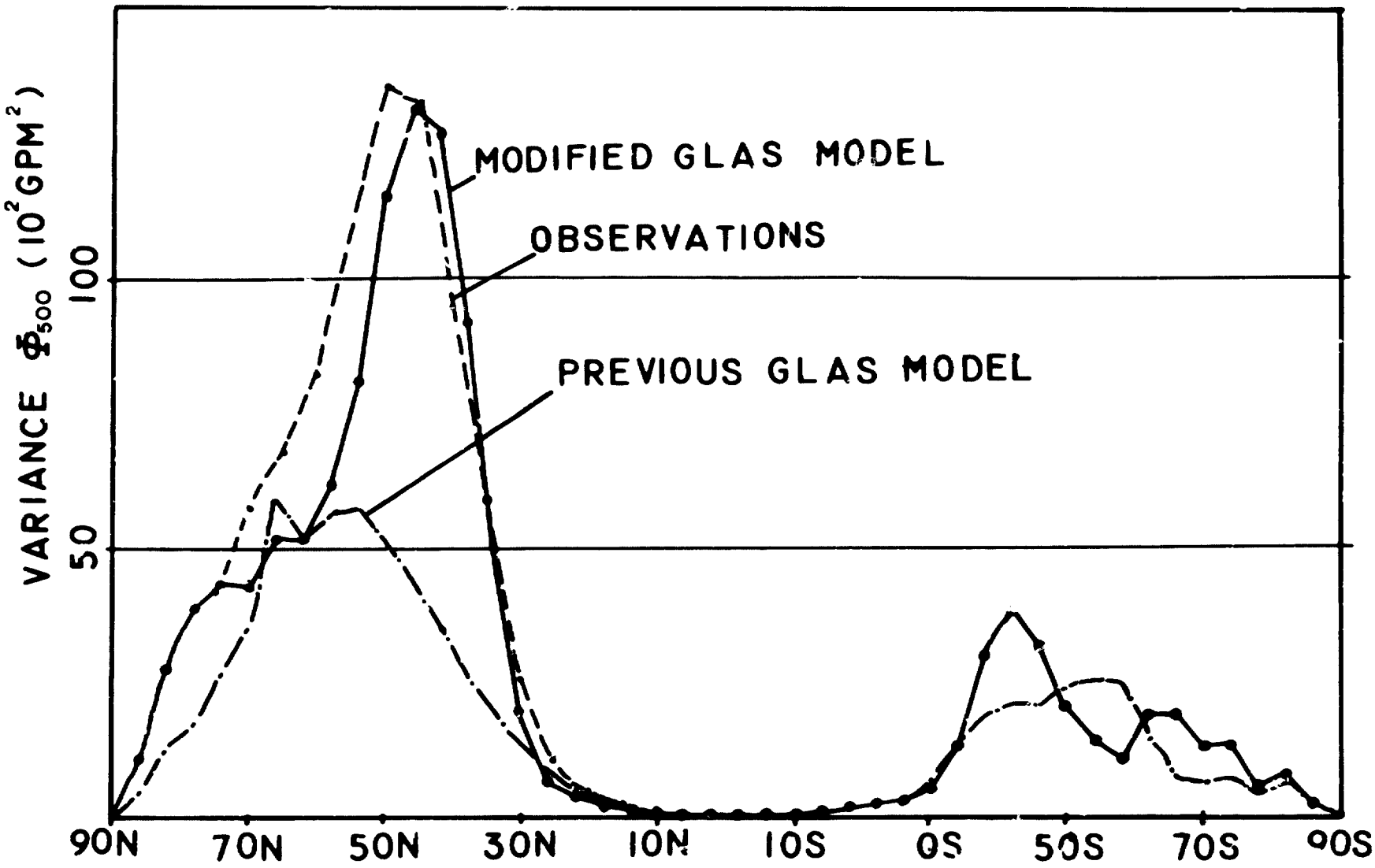

Fig. 11. Stationary variance of January mean geopotential height at 500 mb simulated by two versions of the GLAS climate model, and observations.